Sequential diversification with Miocene extinction and Pliocene speciation linked to mountain uplift explains the diversity of the African rain forest clade Monodoreae (Annonaceae)

Léo-Paul Dagallier, Fabien Condamine, Thomas Couvreur

A sequential diversification with Miocene extinction and Pliocene speciation linked to mountain uplift explains the diversity of the African rain forest clade Monodoreae (Annonaceae)

Léo-Paul M. J. Dagallier[1,2,*], Fabien L. Condamine[3], Thomas L. P. Couvreur[1]

[1] DIADE, Univ Montpellier, IRD, CIRAD, Montpellier, France

[2] Institute of Systematic Botany, The New York Botanical Garden, Bronx, New York 10458, USA

[3] CNRS, Institut des Sciences de l'Evolution de Montpellier (Université de Montpellier), Place Eugène Bataillon, 34095 Montpellier, France

Running title: Macroevolution of Monodoreae in tropical African rain forests

[*] corresponding author: leopauldagallier@gmail.com

Abstract.

- *Background and Aims*: Throughout the Cenozoic, Africa underwent several climatic and geological changes impacting the evolution of tropical rain forests (TRF). African TRF are thought to have extended from East to West in a 'pan-African' TRF, followed by several events of fragmentation during drier climate periods. During the Miocene, climate cooling and mountain uplift led to the aridification of tropical Africa and open habitats expanded at the expense of TRF, which likely experienced local extinctions. However, in plants, these drivers were previously inferred using limited taxonomic and molecular data. Here, we tested the impact of climate and geological changes on diversification within the diverse clade Monodoreae (Annonaceae) composed of 90 tree species restricted to African TRF.

- *Methods*: We reconstructed a near complete phylogenetic tree, based on 32 nuclear genes, and dated using relaxed clocks and fossil calibrations in a Bayesian framework. We inferred the biogeographic history and the diversification dynamics of the clade using multiple birth-death models.

- *Key Results*: Monodoreae originated in East African TRF *ca.* 25 million years ago (Ma) and expanded toward Central Africa during the Miocene. We inferred range contractions during the middle Miocene and document important connections between East and West African TRF after 15–13 Ma. Our results indicated a sudden extinction event during the late Miocene, followed by an increase in speciation rates. Birth-death models suggested that African elevation change (orogeny) is positively linked to speciation in this clade.

- *Conclusion*: East Africa is inferred as an important source of Monodoreae species, and possibly for African plant diversity in general. Our results support a "sequential scenario of diversification" where increased aridification triggered extinction of TRF species in Monodoreae. This was quickly followed by rain forests fragmentation, subsequently enhancing lagged speciation resulting from vicariance and improved climate conditions. In contrast to previous ideas, the uplift of East Africa is shown to have played a positive role in Monodoreae diversification.

Keywords: Annonaceae, aridification, biogeography, birth-death models, diversification, East Africa, forest fragmentation, macroevolution, tropical rain forests

Introduction

Tropical rain forests (TRF) are one of the more biodiverse ecosystems on Earth. Covering just 7% of land, they contain over half of the world's biodiversity (Wilson, 1988; Eiserhardt *et al.*, 2017). After the Amazon basin, the Guineo-Congolian region of Africa contains the second largest continuous extent of TRF in the world (Malhi *et al.*, 2014). The African TRF is divided in two major forested blocks: West-Central and East TRF (Fig. 1; Olson *et al.*, 2001; Couvreur *et al.*, 2008; Droissart *et al.*, 2018; Brée *et al.*, 2020). The West-Central block is divided into two smaller blocks separated by the Dahomey gap located in Benin. The current distribution of TRF across the continent is thought to be the result of various climatic and tectonic events that have shaped the distribution and evolution of African TRF biodiversity (Morley, 2000; Couvreur *et al.*, 2021). A recent review identified six major geo-climatic periods affecting tropical Africa biodiversity evolution (Couvreur *et al.*, 2021). In particular, the Miocene (ca. 23–5.3 million years ago, Ma) is considered crucial in terms of diversification of the African flora (Plana, 2004; Couvreur *et al.*, 2021). For example, the temperature increased during the middle Miocene Climatic Optimum (MMCO, *ca.* 17–14.7 Ma) and TRF expanded across tropical Africa due to warmer and moister climate (Morley, 2000, 2011). Then, from the middle Miocene Climatic Transition (MMCT, *ca.* 15–13 Ma), the global temperatures and *p*CO2 dropped (Zachos *et al.*, 2008; Westerhold *et al.*, 2020). These climate changes, as well as the uplift of East Africa, led to the aridification of Africa throughout the Miocene (Sepulchre *et al.*, 2006; Herbert *et al.*, 2016) favoring the expansion of open, grass-dominated habitats (Retallack *et al.*, 1990; Morley, 2000; Jacobs, 2004; Senut *et al.*, 2009). From 10 Ma, paleo-vegetation records show increasing percentage of C_4 plants until the present (Ségalen *et al.*, 2007; Uno *et al.*, 2016; Polissar *et al.*, 2019) and increases in diversification rates of herbaceous plants like Poaceae and Asteraceae (Kergoat *et al.*, 2018;

Palazzesi *et al.*, 2022), indicating increasing dominance of grasslands across Africa. While open grassland expanded, TRF contracted across its distribution (Plana, 2004). This contraction is suggested to have led to vicariance events within TRF clades before the MMCT, as was detected in several phylogenetic studies (Couvreur *et al.*, 2008; Dimitrov *et al.*, 2012; Menegon *et al.*, 2014; Brée *et al.*, 2020). As drier habitats expanded, some forest-adapted clades experienced habitat shifts towards drier habitats during the Miocene (Davis *et al.*, 2002; Bouchenak-Khelladi *et al.*, 2010; Armstrong *et al.*, 2014; Tosso *et al.*, 2018; Veranso-Libalah *et al.*, 2018). In the early Pliocene (*ca.* 5.3–3.6 Ma), the climate became warmer and moister (Haywood *et al.*, 2013) and the TRF re-expanded while savannas contracted (Morley, 2000; Plana, 2004), suggesting reconnection of West-Central and East TRF blocks (Fer *et al.*, 2017; Joordens *et al.*, 2019).

This climatic changes and rain forest dynamics gave rise to one of the major hypotheses explaining the distribution of TRF plants clades in Africa: the fragmentation-refugia mechanism (Couvreur *et al.*, 2008, 2021; Pokorny *et al.*, 2015). This mechanism links multi-million-year climatic fluctuations and continental wide expansion-contraction of TRF dynamics to numerous vicariant speciation events in TRF-restricted clades (Moritz *et al.*, 2000; Plana, 2004; Loader *et al.*, 2007; Couvreur *et al.*, 2008, 2021). This suggests the existence of a 'pan-African forest' extending continuously from Western to Eastern Africa during favourable climatic times, and fragmenting into isolated Western-Central and Eastern blocks during drier climate periods (Morley, 2000, 2011; Plana, 2004; Couvreur *et al.*, 2021). The fragmentation-refugia mechanism was suggested to explain the present-day distribution patterns of some African TRF clades with species restricted to East or West-Central Africa in plants (Davis *et al.*, 2002; Couvreur *et al.*, 2008; Brée *et al.*, 2020), butterflies (Aduse-Poku *et al.*, 2021), birds (Fjeldså *et al.*, 2007; Fjeldså and Bowie, 2008; Voelker *et al.*, 2010; Huntley

97 and Voelker, 2016; Fuchs *et al.*, 2017), chameleons (Tolley *et al.*, 2013; Nkonmeneck *et al.*,
98 2022), frogs (Bell *et al.*, 2017; Leaché *et al.*, 2019), and mammals (Demos *et al.*, 2014; Bryja
99 *et al.*, 2017; Nicolas *et al.*, 2020). To date, this biogeographic mechanism was inferred based
100 on few data (Couvreur *et al.*, 2008) at the taxonomic and molecular marker sampling level,
101 especially in plants. In particular, the number of vicariant events used to infer this mechanism
102 was generally low (Davis *et al.*, 2002; Couvreur *et al.*, 2008; Brée *et al.*, 2020).

103 Another major hypothesis explaining African TRF diversity is the impact of extinction
104 (Morley and Richards, 1993; Couvreur, 2015). Under the environmental changes, the
105 contraction of the forests did not only trigger speciation via allopatric speciation, but also
106 likely triggered extinction across TRF clades (Morley and Richards, 1993; Plana, 2004;
107 Aduse-Poku *et al.*, 2021). Major extinction events in TRF clades were suggested to occur at
108 the Eocene-Oligocene boundary ca. 33.9 Ma (Pan *et al.*, 2006; Faye *et al.*, 2016; Currano *et*
109 *al.*, 2021), in the first half of the Miocene between 23 and 13.8 Ma (Morley, 2000; Couvreur,
110 2015), in the late Miocene around 11.6 Ma and 7.2 Ma (Morley, 2011) and in the late Pliocene
111 *ca.* 3.6–2.58 Ma (Morley, 2000; Couvreur, 2015). However, signal of past extinction in
112 African TRF plants has rarely been tested with a comprehensive dated phylogeny (e.g. Brée *et*
113 *al.*, 2020).

114 The opposite view to these hypotheses is that speciation and extinction remained relatively
115 constant through time. Indeed, African TRF have lower extant species richness compared to
116 TRF from the Americas and from South-East Asia (Parmentier *et al.*, 2007; Couvreur, 2015).
117 One of the hypotheses invoked to explain such a pattern is that diversification was rather
118 constant in African TRF, whereas American and South-East Asian TRF experienced bursts of
119 speciation (Gentry, 1982; Couvreur, 2015). This hypothesis has been supported by global-

120 scale molecular studies of TRF clades showing no diversification shifts in the African lineages
121 (Erkens *et al.*, 2012; Kissling *et al.*, 2012; Baker and Couvreur, 2013).

122 The bursts of speciation in the American TRF are in part attributed to the Andean uplift
123 (Hoorn *et al.*, 2010; Lagomarsino *et al.*, 2016; Boschman and Condamine, 2022). Indeed,
124 mountain uplift is generally linked to increased diversification, through various mechanisms
125 such as the creation of new habitats or population isolation . These topographic uplifts also
126 have indirect effects via the modification of climate (Sepulchre *et al.*, 2006). In Africa,
127 mountains harbour high levels of species diversity and endemism (Fjeldså and Lovett, 1997;
128 Burgess *et al.*, 2007). East Africa, which has the highest topographical complexity compared
129 to the rest of Africa, has been inferred to be rich in both neo- and paleo-endemics (Dagallier *et*
130 *al.*, 2020). Several geological uplifts occurred during the Cenozoic (Guillocheau *et al.*, 2018;
131 Couvreur *et al.*, 2021), and the uplift of East Africa was documented to occur during the late
132 Miocene (Griffiths, 1993; Sepulchre *et al.*, 2006; Macgregor, 2015; Couvreur *et al.*, 2021).
133 However, the impact of mountain uplift on TRF clade diversification has never been tested.

134 The Monodoreae tribe is an African TRF restricted clade of the plant family Annonaceae. The
135 tribe contains to date 11 genera and 90 species (Dagallier *et al.*, in press) restricted to Africa,
136 with one genus also occurring in Madagascar (*Isolona*). Species distribution in Monodoreae
137 present high levels of endemism across the discrete TRF blocks, occurring either in West-
138 Central or East Africa, with a single species occurring across both blocks (Dagallier, 2021;
139 Dagallier *et al.*, in press). To date, there is little knowledge about the mode of dispersal across
140 the tribe. However, fruit morphology provides some indication about dispersal. Species of this
141 tribe have large fruits (generally larger than 3 cm long), most of them cauliflorous (i.e.
142 growing on the trunk), lack the typical stipe at the base of each individual monocarp
143 composing the fruit in Annonaceae (van Setten and Koek-Noorman, 1992) and are generally

144 dull-coloured, varying from brown, green, or orange. This fruit morphology suggests dispersal
145 syndromes targeting mainly ruminant mammals (Gautier-Hion *et al.*, 1985). Indeed, some
146 studies have shown that species of Monodoreae were included in the diet of TRF understory
147 mammals such as gorillas, chimpanzees, and forest elephants (Gautier-Hion *et al.*, 1985; Tutin
148 and Fernandez, 1993; White *et al.*, 1993; Remis *et al.*, 2001; Rogers *et al.*, 2004).
149 Cauliflorous fruits in particular limit plant dispersal because they target understory dispersers,
150 which are relatively sedentary and habitat specific (Onstein *et al.*, 2018, 2019). Monodoreae
151 are thus unlikely to disperse over long distances i.e. distance such as hundreds or thousands of
152 kilometres, and especially not across different habitats. Finally, very few species have adapted
153 to dry conditions (e.g. *Hexalobus monopetalus*, Botermans *et al.*, 2011) Together, these data
154 suggest that tribe Monodoreae is probably TRF restricted with limited opportunities for long
155 distance dispersal, and thus is a good model to test hypotheses about TRF dynamics through
156 time, in particular the fragmentation-refugia mechanism (Couvreur *et al.*, 2008).

157 Here we infer a near complete species-level dated phylogenomic tree of Monodoreae to test:
158 (1) If the ancestral range of the tribe extended across Africa, supporting the existence of a
159 pan-African rain forest as suggested under the fragmentation-refugia mechanism; (2) If
160 multiple discrete and synchronous speciation events occurred between major forest blocks
161 and if they coincided with increased climatic aridity in Africa leading to TRF fragmentation;
162 (3) If diversification was constant, or if it experienced major increases or decreases of
163 diversification, or sudden extinctions; and (4) If diversification was associated with changes
164 in paleotemperature, proportion of C_4 plants or elevation linked to mountain uplifts.

Material & Methods

Taxon sampling and species distribution

Species delimitation within Monodoreae was previously investigated and validated using a densely sampled phylogenetic tree and morphology (Dagallier, 2021; Dagallier *et al.*, in press). This led to the description of several new species and the placement of two genera into the new tribe Ophrypetaleae. Here, we sampled 88 of the 90 known species of Monodoreae (97.8% of the total species richness). Differences in species number with Dagallier (2021) where 92 species of Monodoreae were reported are due to recent changes: the name *Uvariopsis sessiliflora* is now is a synonym of *U. dioica*, and "*U.* sp nov 1 Uganda" has yet to be formally described due to limited morphological data (Dagallier *et al.*, in press). One specimen per species was sampled, except in the following two cases. In the case of species with described varieties or subspecies, one specimen per variety or subspecies was sampled. Most of the species are geographically restricted to one of the following regions: East Africa, West Africa, Central Africa or West and Central Africa. In the case of species distributed in more than one region, we included one specimen per region when possible. Our dataset also comprised outgroups within the Annonaceae from different closely related tribes, such as the Ophrypetaleae (see Dagallier, 2021; Dagallier *et al.*, in press) and Uvarieae tribes, and from more distantly related tribes (Malmeoideae, Annonoideae). We also included one specimen of genus *Anaxagorea* which is the earliest diverging Annonaceae genus (Couvreur *et al.*, 2019), and one specimen of Eupomatiaceae (*Eupomatia*), which is the sister family of Annonaceae (Sauquet *et al.*, 2003). Details on the vouchers used in this study can be found in Table S1 [**Supplementary Information**]. DNA extractions and library preparations were done

following the protocol described in Dagallier (2021), Dagallier *et al.* (in press) and Couvreur *et al.* (2019). DNA was sequenced on an Illumina HiSeq 2500 with paired reads of 150 pb.

Molecular dataset

For each specimen in our dataset, we retrieved cleaned reads from previous analyses (Dagallier, 2021; Dagallier *et al.*, in press). These reads were then processed and assembled using HybPiper 1.3.1 (Johnson *et al.*, 2016). The reads were aligned to the reference (i.e. the sequences of the 469 nuclear genes targeted) using Burrow Wheeler Alignment (Li and Durbin, 2009) and sorted according to the targeted gene. Reads were then assembled into contigs using SPAdes (Bankevich *et al.*, 2012). Contigs were then aligned to the reference and intron sequences were then generated partially (or completely in case of short introns). Finally, the contigs and the introns were assembled into supercontigs (later also called "genes" or "loci"), i.e. reconstructed genes with multiple exons and partial introns.

The sequences of each gene were then aligned using MAFFT 7.305 (Katoh and Standley, 2013) using the automatic selection of the alignment algorithm (parameter "--auto"). Poorly aligned regions were cleaned using Gblocks 0.91b (Talavera and Castresana, 2007), and the alignments were filled with gaps so that all the sequences in the alignment have the same length and so that every species is included in the alignment. We filtered the dataset to retain only the genes for which the exons sequences mapped at least at 75% of the reference gene and that were retrieved in 75% of the species (75/75 dataset).

HybPiper also includes a tool that flags some of the retrieved genes as potential paralogs in case were different contigs targeted the same reference gene with similar coverage depth (i.e. meaning that variants of the same gene may occur). We executed an exploratory maximum-likelihood phylogenetic reconstruction of these putative paralogs using RAxML 8.2.9

(Stamatakis, 2014), and examined the reconstructed phylogeny to check whether the variants of the genes formed two clear clusters of species. If so, the alignment for this gene was discarded from the dataset.

Using a Bayesian inference (BI) to simultaneously infer phylogenetic relationships and divergence times allows incorporating explicitly topological and age uncertainties. However, the use of BI with hundreds of genes is computationally impossible to achieve in a reasonable time. We thus applied a "gene shopping" approach to select a subset of the most clock-like genes to ease convergence and reduce the computational time (Smith *et al.*, 2018). We first reconstructed a maximum likelihood phylogenetic tree with RAxML for each gene. Each gene tree was then rooted with the outgroup *Eupomatia* using phyx (Brown *et al.*, 2017) and we calculated the root-to-tip variance of the trees using SortaDate (Smith *et al.*, 2018). We then selected a subset composed of the 32 most clock-like genes, that is the 32 genes with the lowest root-to-tip variance. This gene selection strategy has already been used to infer dated phylogenetic trees in Annonaceae (Brée *et al.*, 2020; Helmstetter *et al.*, 2020). Note that we tried with a higher number of genes, but BEAST could not run. For each of these 32 genes, we inferred the best fitting substitution model using ModelTest-NG based on the Bayesian Information Criterion (Darriba *et al.*, 2020).

Phylogenetic reconstruction and molecular dating

We simultaneously reconstructed and dated the phylogenetic tree of Monodoreae using BEAST 2.6.4 (Bouckaert *et al.*, 2019). The alignment of the 32 selected genes (see above) was first converted from fasta to nexus format using PGDSpider (Lischer and Excoffier, 2012) and was assigned a molecular partition in BEAUTi (Bouckaert *et al.*, 2019). Substitution models were defined for each gene following the best model retrieved by

ModelTest-NG (see Table S2 [**Supplementary Information**]) with no estimation of the substitution rate.

To calibrate the molecular clock, we relied on primary fossil calibrations to provide age priors at specific nodes. First, the fossil *Endressinia brasiliana* is a leafy shoot dated from the Aptian-Albian boundary (113.4–112.6 Ma), which confers a maximum age for the crown node of Magnoliineae (i.e. including Annonaceae and Eupomatiaceae) as shown by its phylogenetic placement (Massoni *et al.*, 2015b). Second, the fossil *Futabanthus asamigawaensis* is a flower dated from the early Coniacian (*ca.* 89 Ma) and provides a minimum age for the crown node of Annonaceae (Pirie and Doyle, 2012). We thus constrained the root of the tree (i.e. Annonaceae + Eupomatiaceae) with a hard upper bound at 112.6 Ma and we set a wide uniform prior from 89 to 112.6 Ma on the crown Annonaceae (see nodes marked with orange triangle in Fig. S1 [**Supplementary Information**]).

We set the tree prior as the Yule (pure birth) model, and the clock model as the uncorrelated log-normal (UCLD) model (Drummond *et al.*, 2006) with estimation of the clock rate. We ran 4 Markov chain Monte Carlo (MCMC) in parallel, running for 500 million generations each, sampling every 50,000 generations. We evaluated the convergence of the MCMC with the Effective Sampling Size (ESS) using Tracer 1.7 (Rambaut *et al.*, 2018). We then used TreeAnnotator to draw the Maximum Clade Credibility (MCC) tree, and to compute the mean node ages, the 95% highest posterior density (HPD) of node ages, and the posterior probability (PP) for each node, after discarding the burn-in. We then pruned the dated MCC tree to keep only the Monodoreae tribe and perform the downstream analyses.

Biogeographic history

To reconstruct the ancestral ranges of the Monodoreae and to identify vicariant events, we relied on the Dispersion-Extinction-Cladogenesis (DEC) model (Ree and Smith, 2008) as implemented in the *BioGeoBEARS* R package (Matzke, 2014). We did not run the DEC+J model because founder events (or colonization of new ranges via jump dispersal without intermediate widespread dispersion) are very unlikely in Monodoreae due to their low dispersal abilities (see Introduction), and because DEC+J model inflates the contribution of time-independent cladogenetic events to the likelihood of the model (Ree and Sanmartín, 2018).

First, we assigned each Monodoreae species to a geographical area, corresponding to a TRF region (Fig. 1) in which the species are currently distributed (West Africa, Central Africa, East Africa, or Madagascar). Most of the species were assigned to a single region (endemic range), but some of them were assigned to a widespread range (e.g. West-Central Africa). We restricted the allowed ranges to West (W), Centre (C), East (E), Madagascar (M), West-Centre (WC), Centre-East (CE), East-Madagascar (EM) and West-Centre-East (WCE) and constrained the maximum number of areas per ancestral range to three. We also defined an "area adjacency" matrix in which Madagascar is only adjacent to East-Africa, and defined the dispersal probabilities between areas to one, except for the dispersal probability from and to Madagascar that were set to zero, and the dispersal from East to Madagascar that was set to 0.1.

The marginal probabilities of each range were then plotted on the ancestral nodes and considered the most likely ancestral range as the one having the highest marginal probability. We then considered several biogeographic events to occur at the ancestral nodes. A branch

277 starting at an ancestral node with an endemic range (W, C, E or M) leading to at least one
278 daughter node with a widespread range (WC, CE, EM or WCE) was considered as a range
279 expansion (like “dispersal” in BioGeoBEARS). A branch starting at an ancestral node with
280 widespread range (WC, CE, EM or WCE) leading to one daughter node with an endemic
281 range (W, C, E or M) was considered as a range contraction (“sympatry subset” in
282 BioGeoBEARS). Finally, an ancestral node with widespread range (WC, CE, EM or WCE)
283 leading to two daughter nodes with a different endemic range each (W, C, E or M) was
284 considered as a vicariance event (“vicariance narrow” in BioGeoBEARS). The branches (for
285 range expansion or range contraction events) and nodes (for vicariance events) at which each
286 of these events occurred were then plotted.

287 Diversification analyses

288 Testing for branch-specific and clade-specific diversification rates

289 To test for diversification rate shifts across the reconstructed tree, we used three different
290 methods designed to estimate the branch-specific or clade-specific speciation and extinction
291 rates. The net diversification rate is defined as speciation minus extinction (later referred as
292 “diversification rate”). The use of several different models allows to cross-check the
293 estimations (Condamine *et al.*, 2018). Nonetheless, it is worth mentioning that each method
294 differs at several points in the way speciation and extinction rates are estimated.

295 First, we used the cladogenetic diversification rate shift (ClaDS) model to estimate branch-
296 specific diversification rates. ClaDS implements a birth-death model where speciation rates
297 are inherited at a speciation event, but with a shift drawn from a probability distribution
298 parameterized with the parental rates (Maliet *et al.*, 2019). The extinction rate also varies

across branches, but the turnover (that is speciation divided by extinction) is constant across the branches. The model is then computed using data augmentation in a MCMC with 3 chains. To assess convergence, the Gelman statistics are then computed every 200 iterations and the chains stop when these statistics drop below 1.05. We used the ClaDS model as implemented in the PANDA Julia package (Maliet and Morlon, 2021).

Second, we used RevBayes to model the estimation of branch-specific diversification (speciation and extinction) rates (BSDR; Höhna *et al.*, 2019). The BSDR model is a birth-death model that breaks time into small intervals and for which speciation and extinction rates can change at each time interval. The new speciation and extinction rates at a new interval are drawn from a lognormal distribution. To ease the computation, the lognormal distribution is approximated using discrete rate categories. We set up the model following the RevBayes tutorial (available at: https://revbayes.github.io/tutorials/divrate/branch_specific.html). The parameters were then estimated using two reverse-jumping Markov Chain Monte Carlo (rjMCMC) of 4'000 iterations each, sampling every 200 iterations. We performed several analyses with different sets of priors to check the consistency of the results between the different prior specifications. We set the discrete rate categories prior to 6 or 10, and the initial value of the number of expected rate shift to 1, 4 or 10. The convergence of the rjMCMC was checked with ESS above 200 using Tracer 1.7 (Rambaut *et al.*, 2018).

Third, we used the Bayesian analysis of macroevolutionary mixtures (BAMM) to estimate the variation of speciation and extinction rates through time, but also to detect significant clade-specific shifts in these rates (Rabosky, 2014). BAMM uses reversible-jump Markov Chain Monte Carlo (rjMCMC) to explore the space of parameters and the number of rate shifts. We set prior values using the *BAMMtools* R package (Rabosky *et al.*, 2014), with an expected number of rate shifts equal to 1. We ran four rjMCMC for 10'000'000 generations, sampling

every 10’000 generations. We then calculated the ESS of the log-likelihood and the number of shifts using the *coda* R package (Plummer *et al.*, 2020) after discarding 10% of burn-in to assess the convergence of the chains (ESS > 200).

Each of these three models account for the sampling fraction in the calculation of the parameters. For ClaDS and BAMM, we set the sampling fraction to be clade specific, with every genus fully sampled (i.e. a sampling fraction of 1) except for *Uvariopsis* and *Lukea* having a sampling fraction of 0.85 and 0.5, respectively. For the BSDR model, we set the sampling fraction for the whole phylogeny at ca. 0.978.

Testing for sudden extinction events

To test whether the evolutionary history of the Monodoreae was impacted by one or several sudden extinction events, we used the compound Poisson process on Mass-Extinction Times model (CoMET; May *et al.*, 2016) as implemented in the *TESS* R package (Höhna *et al.*, 2016). This model estimates the tree-wide speciation and extinction rates, and the probability of several tree-wide events to occur such as shifts in speciation rate, shifts in extinction rates, or sudden extinction events, i.e. when several lineages go extinct with a prior probability. The speciation and extinction rates are constant between two events. The events are estimated under the independent compound Poisson process. Parameters are estimated using a reverse jump MCMC (rjMCMC) over various episodic birth-death models. Model confidence is assessed by computing the Bayes factors (BF) between each model (May *et al.*, 2016). For our CoMET analysis, we set the priors on the number of extinction event and number of expected changes to 2. Note that the prior on the number of events does not impact the results as the models are compared using BF (Höhna *et al.*, 2015). We performed 10 different CoMET analyses with prior values on the survival probability to an extinction event ranging

every 5% from 5% to 50%. The rjMCMC was run until the ESS for each parameter reaches at least 500. We considered the support for a rate shift or for a ME event as substantially significant for 2lnBF > 2, as strongly significant for 2lnBF > 6 and as decisive for 2lnBF > 10 (Kass and Raftery, 1995; Höhna *et al.*, 2015).

Testing the impact of the paleoenvironment

To test if the diversification of the Monodoreae was associated with changes in past environmental variables (temperature, elevation variation of the African continent, and proportion of C_4 plants in the African paleoflora), we fitted several birth-death models that estimate the speciation and extinction rates along a continuous time in a maximum-likelihood framework. We set the models allowing the speciation and extinction rates to vary exponentially with time (time-dependent models) or exponentially with environmental variables (environment-dependent models) (Condamine *et al.*, 2013). We also fitted models with constant or null speciation and extinction rates. The best fitting model was then evaluated using the corrected Akaike Information Criterion (AICc). The complete list of models fitted is given in Table 1.

The environment-dependent models use environmental data spanning the time interval covered by the phylogenetic tree. Missing values were interpolated using the spline interpolation implemented in the sm.spline function from the *pspline* R package (Ripley, 2017). Past temperature at global scales was inferred from the widely used oxygen isotope data recovered from benthic foraminifer shells (Zachos *et al.*, 2008; Westerhold *et al.*, 2020). Past elevation change across the African continent was newly computed using the data from Scotese & Wright (2018). First, the geo-referenced occurrences of the Monodoreae species were extracted from the RAINBIO database (Dauby *et al.*, 2016), and the convex hull

containing all the point coordinates was computed using the chull function from the *grDevices* R package. After conversion to SpatialPolygonsDataFrame object with the *sp* R package (Pebesma *et al.*, 2021), the intersection of the envelope with the African coastline was computed using *gIntersection* function in the *rgeos* R package (Bivand *et al.*, 2020). Within this intersected envelope, we computed the geo-coordinates of every unique point with latitude and longitude values at one degree precision (e.g. points with coordinates 10°N 10°E, 10°N 11°E, 10°N 12°E, etc.), and extracted the elevation value for each of these points every 5 Myr (million years) from the present to 30 Ma, using the reconstruct function in the *chronosphere* R package (Kocsis and Raja, 2021). We then computed the mean elevation for each time.

Finally, the proportion of C_4 plants in the African paleoflora is taken from the reconstructions made by Pollisar *et al.* (2019) based on the composition of ^{13}C isotope in plant waxes. To represent the proportion of C_4 plants in tropical Africa, we selected the data from the sites 959 (Guinean Gulf), 241 and 235 (East Africa). Given the oldest C_4 value at 23.38 Ma is very low compared to the values from 15 to 20 Ma (1.66 vs. 10.69 – 13.05), we replaced it by the lowest value found between 15 and 20 Ma (that is 10.69) to avoid distortion of the interpolation toward negative values. Moreover, as 23.38 Ma is younger than the clade age (25 Ma), we artificially duplicated the 10.69 a C_4 value at 25.1 Ma (Fig. S17 [**Supplementary Information**]).

The scripts for the biogeographic and diversification analyses carried out in this study are available at https://github.com/LPDagallier/Monodoreae_macroevolution.

Results

Gene recovery

We recovered all the 369 exons, at least partially, targeted by the Annonaceae bait kit (Couvreur *et al.*, 2019). After filtering and removal of the paralogous loci, the 75/75 dataset contained 318 supercontigs. The 32 supercontigs most clock-like used for the phylogenetic reconstruction and dating had a length comprised between 509 and 4,796 bp. Their best substitution models are listed in the Table S2 [**Supplementary Information**].

Phylogeny

Among the six independent MCMC runs with a Yule tree prior, only one fully converged to a likelihood of -399,351.6164 after discarding 14% of burn-in (ESS for all the parameters above 200 after discarding the burn-in). The other chains were converging toward a slightly higher likelihood value, but the ESS values for several loci, for the prior and for the Yule model was below 150. After discarding the burn-in, the MCC tree was estimated from 8,601 posterior trees. All the nodes in the MCC tree show strong support with all the nodes having a posterior probability (PP) of 1, except for two nodes having a PP > 0.9 (Fig. 2). All the genera were retrieved monophyletic.

The mean age of the divergence between the *Eupomatia* (outgroup) and the Annonaceae (i.e. the crown node of Magnoliineae) is estimated in the Early Cretaceous at 110.68 Ma (95% HPD: 105.53–112.60 Ma). The crown node of Annonaceae is estimated in the Late Cretaceous at 89.87 Ma (95% HPD: 89.00–92.55 Ma) (Fig. S1 [**Supplementary Information**]). Although the distribution probabilities of the calibration points set on these nodes were broad uniforms, the age estimates for the crown node of Monodoreae and the

crown node of Annonaceae have respectively converged to the lower and upper bounds of the prior distribution. This indicates that the data contain enough information to overcome the lack of precise information of such wide priors. The age of the Monodoreae tribe is estimated in the late Oligocene at 25.07 Ma (95% HPD: 22.52–27.30 Ma) (Fig. 2).

Biogeographical events

The DEC analysis estimated the rate of 'dispersal' (range expansion) to 0.039 events/lineage/Myr and the rate of 'extinction' (range contraction) to 0.008. East Africa was identified as the most likely geographic origin of the Monodoreae (Fig. 3), as well as for most of the ancestral nodes until *ca.* 15 Ma. The ancestral range of *Hexalobus*, *Isolona*, *Mischogyne*, *Monodora*, and *Uvariopsis* was likely widespread (Centre-East or West-Centre-East), the ancestral range of *Asteranthe*, *Lukea* and *Uvariodendron* was likely East Africa, while the ancestral range of *Uvariastrum* was likely Central Africa. Between the origin and *ca.* 13.5 Ma, the range of the Monodoreae expanded, and from *ca.* 13.5 to 6.5 Ma the range of some taxa contracted while the range of some other taxa possibly expanded (Fig. 4). From the late Miocene (*ca.* 6.5 Ma), the Monodoreae underwent several synchronous range expansion events, range contraction events and vicariance events. Within Monodoreae, a single dispersal event occurred from East Africa to Madagascar in the genus *Isolona* dated between 5.27 and 4.14 Ma. This led to a founder event followed by a small radiation with five known Malagasy species (Fig. 3). Interestingly, the DEC model retrieved this divergence as a vicariance event (Fig. 3). However, as Madagascar had already separated from mainland Africa, it seems unlikely that the ancestor (node 153, Fig. S1 [**Supplementary Information**]) was distributed in both East Africa and Madagascar. We thus interpret this event as a founder event (Fig. 4).

Diversification analyses

Branch-specific and clade-specific diversification rates

The three methods used in our study identified to various degrees changes in the speciation and extinction rates across Monodoreae and its genera. Nevertheless, BAMM did not detect any significant diversification rate shifts across the phylogeny (Fig. S5, Fig. S6 [**Supplementary Information**]). ClaDS inferred low speciation rates in the species-poor (5 species or less) genera *Asteranthe*, *Hexalobus*, *Lukea*, *Mischogyne* and *Uvariastrum*, and relatively high speciation rates in one of the most diverse genera *Uvariopsis* (Fig. 5). RevBayes estimated higher speciation rates around the crown of the genera *Isolona*, *Monodora*, *Uvariodendron* and *Uvariopsis* (Fig. S3a [**Supplementary Information**]). The variation of the speciation rate estimated by BAMM was very low, from 0.17 event/lineage/Myr around the root of the phylogeny to 0.2 event/lineage/Myr in the genus *Uvariopsis* (Fig. S4a [**Supplementary Information**]). These three methods estimated very low extinction rates (less than 0.03 event/lineage/Myr; Fig. S2, Fig. S3b, Fig. S4b [**Supplementary Information**]). The three methods have also in common higher diversification rate in the genus *Uvariopsis*.

Tree-wide diversification rates

Even when using different priors on the survival probability of a sudden extinction event, the different CoMET analyses return similar results (Fig. S7 – Fig. S16 [**Supplementary Information**]). CoMET found the speciation rate to vary through time: speciation is rather constant at around *ca.* 0.2 event/lineage/Myr until *ca.* 7 Ma, then increases to around 0.35 event/lineage/Myr between 6.5 and 4 Ma, and finally drops after 4 Ma to below 0.15

event/lineage/Myr (Fig. 6), which corresponds to the detected shifts (see below). The extinction rate is inferred to be rather low and constant through the history of the tribe (Fig. S7 – Fig. S16 [**Supplementary Information**]). CoMET detected a speciation rate shift increase with substantial (2lnBF > 2) to strong (2lnBF > 6) support between 6.5 and 7 Ma, followed by a speciation rate shift decrease between 2.5 and 4.25 Ma with substantial support, and a final shift towards even lower speciation rates around 1 Ma with strong support (Fig. 6). CoMET also identified several extinction events with substantial support in the late Miocene (between 10 and 6.5 Ma), with a strong support between 6 and 6.25 Ma when the survival probability was less than 10% (Fig. 6).

Paleoenvironmental birth-death models

The environmental birth-death model with the lowest AICc score is the BDPerC4 model (4 parameters), which is a model with speciation and extinction rates varying exponentially with the proportion of C_4 plants through time (Table 1). However, the estimated parameters for this model are unrealistic as the inferred diversification rate is negative (i.e. extinction rate higher than speciation rate) at the beginning of the clade's history, which is biologically implausible. The second-best model is the BElev model (2 parameters), which is a model with speciation rate varying with mean elevation in tropical Africa through time and no extinction (Table 1, Fig. 7). Note that the difference of AICc between BElev and the BElevDConst (speciation varying with elevation through time and constant extinction) is low, but these two models are very similar as the constant extinction rate estimated for the BElevDConst is 0.005 events/lineage/Myr (Table 1).

Discussion

In this study we generated a near complete species-level dated phylogenomic tree for a diverse rain forest restricted clade of pan-African and Madagascar trees. Using this framework, we tested several hypotheses linked to the biogeography and diversification history of rain forests across the continent throughout the Miocene (last 23 Myr). We used BEAST to co-estimate the phylogeny and the divergence times in BEAST, however using a subsample of the molecular markers available (32 most clocklike markers). The resulting phylogenetic tree is topologically very similar to the one obtained using the full set of molecular makers except for some nodes (mainly in *Isolona*, *Monodora* and *Uvariastrum*) for which gene trees conflict was inferred using both concatenation and gene trees approaches (Dagallier *et al.*, in press). Reticulate processes of evolution might occur at these nodes, and the selection of only 32 loci for the molecular dating might increase the bias towards one or the other topology. One notable difference is the position of *Monodora minor*, which was inferred as sister to the genus with strong support using the full dataset (Dagallier, 2021; Dagallier *et al.*, in press) but is recovered nested within the genus with moderate support in this 32-marker dataset using BEAST (Fig. 2).

East African origin and biogeography of Monodoreae

Our biogeographic analysis inferred East Africa as the most likely ancestral area for the tribe (Fig. 3). Indeed, the East African restricted genera *Asteranthe* or *Lukea* are recovered as sister to the more widely distributed clades. At the genus level, East African endemic species are generally recovered as sister to the rest of the genus (*Isolona linearis*; *Uvariodendron mbagoi*; *Monodora minor*, see above for the later), although not always (*Uvariopsis*). This scenario contrasts with other TRF groups inferred to have originated in Central Africa before

dispersing to East Africa (e.g. Davis *et al.*, 2002; Brée *et al.*, 2020; Aduse-Poku *et al.*, 2021). Interestingly, within Annonaceae, several other East African endemic genera are recovered as sister to different tribes such as *Mkilua fragrans*, sister to the rest of Bocageeae (Couvreur *et al.*, 2011a), and the two monotypic endemic genera *Sanrafaelia* and *Ophrypetalum*, sister to the diverse paleotropical tribe Uvarieae (Dagallier, 2021; Dagallier *et al.*, in press). East African rain forests are thus not only important in terms of species diversity and endemism (Couvreur *et al.*, 2006), but could also potentially contain a unique and old evolutionary history within Annonaceae, stressing there importance for conservation.

The most recent common ancestor of extant Monodoreae (crown node) is dated to 25 Ma, during the late Oligocene (Fig. 2). Initially, it was suggested that Monodoreae originated just before the Eocene–Oligocene Transition (EOT, 33.9 Ma), however this was based on plastid markers that included the monotypic genera *Sanrafaelia* and *Ophrypetalum* in Monodoreae (Couvreur *et al.*, 2008; Chatrou *et al.*, 2012). Based on the analyses of hundreds of nuclear markers both genera are now recovered as sister to tribe Uvarieae and have been transferred to their own tribe: Ophrypetaleae (Couvreur *et al.*, 2019; Dagallier, 2021; Dagallier *et al.*, in press), leading to a 7 Myr younger crown node age for Monodoreae. The late Oligocene (29-24 Myr) was a time of relatively favourable conditions for TRF, re-expanding after the EOT crisis (Couvreur *et al.*, 2021). Although the interpretation of East African ecosystems at that time is complex (Jacobs *et al.*, 2010; Linder, 2017), TRF-like vegetation is clearly documented in northern Ethiopia (Jacobs *et al.*, 2005, 2010; Bonnefille, 2010; Pan, 2010; Currano *et al.*, 2011) and in northern Kenya as mosaics of TRF and semi-deciduous forests (Vincens *et al.*, 2006). The inferred age of Monodoreae also fits well with the origin of several other animal TRF clades underling the importance of the late Oligocene in the origin of African rain forest biodiversity (Couvreur *et al.*, 2021).

From East Africa, our biogeographic analysis suggests several range expansions of Monodoreae into Central Africa becoming widespread during the early to middle Miocene (*ca.* 24–13.5 Ma) (Fig. 3 and Fig. 4, range expansion, green). Given the low potential for long-distance dispersal of this tribe, our results support the hypothesis of important TRF East/Central connections possibly via the existence of a continuous pan-African rain forest (Couvreur *et al.*, 2021; but see Linder 2017 for a counter argument about the existence of a pan-African forest, and below). Indeed, this coincides with the warmer climate of the MMCO (*ca.* 17–14.7 Ma) during which the TRF was suggested to occur from coast to coast (Morley, 2000, 2011; Couvreur *et al.*, 2021). It is during the early Miocene (*ca.* 20–21 Ma) that the genera *Asteranthe* and *Lukea* originated (Fig. 3). These genera are species poor (two species each) and are endemic to East African coastal and mountain forests (Verdcourt, 1971; Vollesen, 1980; Cheek *et al.*, 2022). Such long-term persistence of clades originating in the Oligocene-Miocene has also been documented in plants and animals (Tolley *et al.*, 2011; Dimitrov *et al.*, 2012; Loader *et al.*, 2014; Couvreur *et al.*, 2021), and is associated with potential climate stability of the region in the East African mountains region (Lovett *et al.*, 2005; Finch *et al.*, 2009). The divergence between *Asteranthe* and the clade *Hexalobus* – *Uvariastrum* was interpreted as a vicariance event *ca.* 16.8 Ma by Couvreur *et al.* (2008). Here, with a full taxon sampling of these genera, we rather estimate a range expansion from the East to East-Centre *ca.* 20.7 Ma with a long-term persistence of the genus *Asteranthe* in the East. This period still coincides with warmer and wet climates across Africa, even though the existence of continuous TRF between East and West Africa remains debated (Jacobs *et al.*, 2010; Linder, 2017; Couvreur *et al.*, 2021).

Just after the MMCO, during the MMCT (*ca.* 15–13 Ma), global temperatures and *p*CO2 dropped (Westerhold *et al.*, 2020) leading to the expansion of open grasslands across Africa

548 and contraction of TRF (Jacobs, 2004; Plana, 2004; Linder, 2017; Couvreur *et al.*, 2021).
549 Previous molecular studies postulated vicariance events in TRF restricted clades before the
550 MMCT, supporting the contraction of the TRF during the MMCT (Couvreur *et al.*, 2008;
551 Dimitrov *et al.*, 2012; Menegon *et al.*, 2014; Brée *et al.*, 2020). However, in Monodoreae, we
552 did not find evidence of vicariance (i.e. splitting of one species into two) before 6 Ma (Fig. 4).
553 Rather, our results support a range contraction scenario (i.e. the disappearance of a species
554 from part of its past range) from *ca.* 13.5 to 6.5 Ma (Fig. 4), leading to the origins of
555 *Uvariodendron* in East Africa, *Uvariastrum* in Central Africa and corresponding to the
556 divergence between the East African species *Isolona linearis* and the rest of *Isolona* (Fig. 3).
557 Even if these clades evolved in isolation, and would support for a contraction of the TRF at
558 that time, their sister clades are inferred as widespread (i.e. distributed across both East and
559 Central Africa, Fig. 3). Moreover, possible range expansions also continued between *ca.* 13.5
560 and 6.5 Ma (Fig. 4). Overall, these results support the idea that the East and Central African
561 TRF might have been more connected than previously suggested after the MMCT. Indeed, as
562 noted by Jacobs (2010), numerous paleofloras of the middle Miocene of East Africa document
563 the presence of taxa sharing affinities with both wet and dry forests of Central and West
564 Africa. A striking example is that of Baringo in the Ngorora Formation in the East African
565 Rift valley (west Kenya; *ca.* 12.2 Ma), inferred as being a moist to wet forest containing
566 several tropical plant lineages, including Annonaceae, and several taxa were suggested to
567 have affinities with modern West African species (Jacobs *et al.*, 2010). Also, as the
568 Monodoreae experienced sudden extinction in the late Miocene (see below), we might miss
569 the ancestral ranges of the extinct (and unknown) species, which may overshadow the signal
570 inferred by DEC between two nodes separated by a long branch.

From the late Miocene and during the Pliocene (6.5–2 Ma), the biogeographic history of the Monodoreae increases in complexity. First, most of the extant Monodoreae species diverged during this time interval (Fig. 2, Fig. 3) supporting evidence of the importance of this period for the origin of African biodiversity (Voelker *et al.*, 2010; Couvreur *et al.*, 2021). Second, our biogeographic analysis resulted in numerous simultaneous range expansions, contractions and vicariance events (Fig. 4). This suggests that if TRF fragmentation events occurred, it was not strong enough to affect the whole tribe. Instead, the TRF blocks were likely connected during the early Pliocene, as previously suggested based on paleo-vegetation record (Morley, 2000), either as a continuous forest block (Fer *et al.*, 2017) or via forested corridors between East and Centre-West Africa (Joordens *et al.*, 2019). Thus, the late Miocene and Pliocene divergences in the Monodoreae might be explained by species-specific or region-specific mechanisms.

Although most species of Monodoreae are restricted to rain forests, a few isolated species have adapted to dry conditions. The two sister species, *Hexalobus monopetalus* and *H. mossambicensis*, are more dry-adapted than the other *Hexalobus* species distributed in Central Africa (Botermans *et al.*, 2011), and *H. monopetalus* has the typical savanna distribution all around the Guineo-Congolian region (Botermans *et al.*, 2011) like other savanna species (Lehmann *et al.*, 2011; Gonçalves *et al.*, 2021). In addition, *Monodora stenopetala* (Couvreur, 2009) and *Uvariastrum hexaloboides* (Couvreur, 2014) are also reported to be dry adapted both occurring in woodlands or dense thickets of southern East Africa. These species, shifting from a forested and wetter to a drier and more open habitat, were estimated to have originated during the late Miocene between 6 and 3 Ma (Fig. 2). These three independent habitat shifts followed by little or no speciation contrasts with other plant clades for which multiple shifts into drier habitats followed by speciation have been documented during the late Miocene,

595 such as in the African Melatsomataceae (Veranso-Libalah *et al.*, 2018), Cucurbitaceae
596 (Holstein and Renner, 2011), Fabaceae (Bouchenak-Khelladi *et al.*, 2010; Tosso *et al.*, 2018),
597 and Sapotaceae (Armstrong *et al.*, 2014). This supports the view that Annonaceae show little
598 ecological capacity to adapt to drier more arid conditions in Africa in line with previous
599 results (Couvreur *et al.*, 2011b).

600 Several Monodoreae species span both West and Centre TRF blocks (Fig. 2, Fig. 3). The
601 Dahomey Gap (DG) located in Benin and Togo mediates the connection between the West
602 and the Central African forests blocks (Droissart *et al.*, 2018). The DG was suggested to be
603 dominated by open vegetation during most of the late Quaternary, from *ca.* 1.05 Ma
604 (Demenou *et al.*, 2018), and became forested during the mid-Holocene (*ca.* 8000–4000 years
605 before present), before being dominated again by open vegetation until the present due to
606 climatic variations (Salzmann and Hoelzmann, 2005). These vegetation changes show
607 signatures in the intraspecific genetic structure of many forest trees species (Duminil *et al.*,
608 2015; Demenou *et al.*, 2018, 2020; Lompo *et al.*, 2018). In this study, we dated the
609 intraspecific divergence times of eight species co-occurring west and east of the DG (one
610 individual per side sampled). For three of these species (*Monodora myristica*, *Uvariastrum*
611 *pierreanum* and *Uvariodendron calophyllum*), divergence times were estimated to the late
612 Quaternary (i.e. after 1.05 Ma) (Fig. 2). In addition, no *interspecific* vicariance events
613 between West and Centre species were inferred during this period (Fig. 3, Fig. 4), suggesting
614 that the presence of the DG acted as a barrier only for genetic differentiation in these species
615 as is generally reported (Couvreur *et al.*, 2021). We also inferred infraspecific divergence
616 times prior to 1.05 Ma spanning 6.57 and 1.20 Ma associated to inter- and intraspecific
617 vicariance and range expansion events between the West and Central TRF blocks (Fig. 2, Fig.
618 3, Fig. 4). This result agrees well with the scenario of multiple expansion and retractions of

savannah vegetation in West Africa, connecting and disconnecting rain forests between West and Central Africa throughout the last 7 Myrs (Bonnefille, 2010; Jacobs *et al.*, 2010). In particular, the climatic variations in the Pliocene and the early Pleistocene (mainly glacial and interglacial cycles, Couvreur *et al.*, 2021) triggered strong isolations in some populations, leading to splits between West and Central African species (e.g. origin of *Isolona deightonii*, *Uvariopsis guineensis*, or *Uvariopsis oligocarpa*), but also seem to allow the re-connection of the populations of some species both distributed in West and Central Africa (e.g. *Monodora undulata*, *Dennettia tripetala*). A similar pattern with both inter- and intraspecific divergence between West and Centre Forest blocks has been observed during the Pliocene and Pleistocene in the bird genera *Bleda* and *Criniger* (Huntley and Voelker, 2016; Huntley *et al.*, 2018).

Madagascar broke apart from Africa in the Early Cretaceous (more than 100 Ma; Kocsis & Scotese, 2021) and the shortest distance today separating the African coast to Madagascar is *ca.* 400 km (Rabinowitz and Woods, 2006). Similar recent splits between Malagasy clades and continental relatives have been inferred in animals and plants (Renner, 2004; Rabinowitz and Woods, 2006; Yoder and Nowak, 2006; Tolley *et al.*, 2013), including other Annonaceae (Thomas *et al.*, 2015; Chen *et al.*, 2019), and have generally been explained by long-distance dispersal (LDD). Small vertebrates and invertebrates are hypothesized to have drifted on vegetation rafts from continental African rivers with the help of eastwards oceanic currents (Rabinowitz and Woods, 2006; Ali and Huber, 2010). LDD from the continent to Madagascar is likely in wind-dispersed plant species and is also documented in bird-dispersed plants species (Renner, 2004; Yao *et al.*, 2016). *Isolona* is the only Monodoreae genus that reached Madagascar. We estimated that this event happened during the early Pliocene between 5.27 and 4.14 Ma followed by a small radiation of five species (Fig. 3, Fig. 4). The timing of this

643 dispersal occurs on the more recent timeline of endemic plant lineage origins in Madagascar
644 which span the middle Eocene/Oligocene till the Pleistocene (Buerki *et al.*, 2013; Antonelli *et*
645 *al.*, 2022). The fruits of *Isolona* are large syncarps probably dispersed by large to medium-
646 bodied primates (Couvreur, 2009), and terrestrial LDD is considered unlikely in this genus
647 (Couvreur *et al.*, 2008). To explain the presence of *Isolona* in Madagascar, we speculate that
648 some propagules (fruits, seeds, or seedlings) derived from mainland rivers in East Africa to
649 the ocean and reached Madagascar by drifting via an eastward oceanic current. This is
650 supported by the fact that the sister species to the Malagasy clade is *Isolona heinsenii*
651 endemic to the East African rain forests in Tanzania (Verdcourt, 1971; Couvreur, 2009;
652 Dagallier, 2021; Dagallier *et al.*, in press). Dispersal by drifting to Madagascar is suggested as
653 the main hypothesis for the origin of Malagasy biodiversity (Yoder and Nowak, 2006; Buerki
654 *et al.*, 2013; Antonelli *et al.*, 2022), and has also been suggested in the paleotropical
655 Annonaceae genus *Uvaria*, for which the African species are also unlikely to disperse across
656 the ocean (Zhou *et al.*, 2012). Although seed survival of *Isolona* (and Monodoreae in general)
657 in salted water remains unknown, it is possible that some propagules survived during the
658 crossing, especially if they drifted on rafts of vegetation detached from East Africa (Ali and
659 Huber, 2010). An alternative hypothesis could be that the propagules of an ancestral *Isolona*
660 species reached Madagascar via land bridges linking Africa and Madagascar (e.g. Masters *et*
661 *al.*, 2021) and allowing different animal migrations, notably at three distinct moments during
662 the Cenozoic, including the Miocene (12—5 Ma). However, viable land bridges across the
663 Mozambique Channel were shown to be very unlikely (Ali and Huber, 2010; see Ali and
664 Hedges, 2022 for a review). In addition, crossing the channel even when the sea level was low
665 is also improbable, given that the bathymetry is deep, and even a drop of 200 m would only
666 reduce the distance between the continent and Madagascar to 360 km (Rabinowitz and
667 Woods, 2006). Finally, the presence of *Isolona* in Madagascar was used as a counter argument

668 to our assumption of low potential for LDD of Monodoreae species (Linder, 2017). However,
669 this successful dispersal event occurred only once throughout the evolutionary history of
670 Monodoreae and should thus be viewed as additional proof of the low LDD capacity of the
671 species in this tribe, not the opposite.

672 Diversification of the Monodoreae

673 Speciation rates for Monodoreae, as inferred with CoMET, were relatively stable until the late
674 Miocene some 10 Mya (Fig. 6). The first event detectable with our data was a sudden
675 extinction occurring during the late Miocene between 10 and 6.5 Ma (Fig. 6, Fig. S7 – Fig.
676 S16 [**Supplementary Information**]). Similarly, Brée *et al.* (2020) found substantial support
677 in favour of a sudden extinction around the same time, between 8 and 6.5 Ma in the
678 Piptostigmateae, another TRF African Annonaceae tribe, although they do not consider it
679 significant (see Fig. 4 in Brée *et al.*, 2020). This pattern has also been retrieved in the African
680 butterfly genus *Bicyclus* for which the forest clade underwent a drop in diversification rate
681 from ca. 15 Ma (Aduse-Poku *et al.*, 2021). These results are consistent with the late Miocene
682 Cooling suggested to have increased aridification across Africa leading to the expansion of
683 open grasslands (Jacobs, 2004; Uno *et al.*, 2016; Couvreur *et al.*, 2021), although this trend
684 was not homogenous through time or space (Jacobs, 2004; Bonnefille, 2010). This supports
685 growing evidence that the open grasslands in the late Miocene occurred at the expense of the
686 TRF, which might have experienced drastic and sudden extinction due to the reduction of
687 areas having a suitable warm and wet climate (Morley, 2000, 2011).

688 Interestingly, using two different methods (CoMET and the environment-dependent
689 diversification model) our results indicate that this sudden extinction event was immediately
690 succeeded by a potential increase in speciation rates dated to have taken place between 6.5

691 and 4.25 Ma (Fig. 6, Fig. 7 Fig. S7 – Fig. S16 [**Supplementary Information**]). This increase
692 coincided with the early Pliocene which was marked by a renewed warmed climate across
693 Africa (Jacobs *et al.*, 2010; Couvreur *et al.*, 2021). Our biogeographical analysis identifies
694 numerous vicariance events between major regions also dating to the early Pliocene (Fig. 4).

695 In addition, the model with change of elevation through time best explained the speciation
696 rate with no extinction in Monodoreae (BElev model; Fig. 7; Table 1, but see Results). This is,
697 to our knowledge, the first time African elevation change (orogeny) is positively linked to
698 speciation in an African rain forest tree clade. The timing of the orogeny of the East African
699 Rift System is complex (Chorowicz, 2005; Ring *et al.*, 2018; Couvreur *et al.*, 2021), but our
700 results would fit with an active phase of uplift suggested to occur along the Western branch
701 around 15 to 10 million years ago (Chorowicz, 2005; Wichura *et al.*, 2015; Ring *et al.*, 2018).
702 The rise of the East African Rift has generally been interpreted as having a negative impact of
703 African rain forest biodiversity leading to precipitation reduction and the drying of the Congo
704 basin for example (Sepulchre *et al.*, 2006; Sommerfeld *et al.*, 2016). However, rifting in East
705 Africa could have led to the fragmentation or complete genetic isolation of both East and
706 West/Central Forest blocks favouring vicariance (Fig. 4).

707 Taken together, our results suggest that both aridification and rifting initially had a negative
708 impact of TRF diversity but was quickly followed by an increase in speciation linked to
709 vicariance. We suggest here a “sequential scenario of diversification” starting with an
710 increased aridification triggering extinction of TRF taxa followed by the fragmentation of rain
711 forests resulting from rain fall reduction subsequently enhancing lagged speciation events
712 resulting from vicariance and improved climate conditions.

Uvariopsis, an outlier in the diversification of Monodoreae?

At the clade level, our BAMM analyses failed to detect any significant shifts in diversification rates across Monodoreae (Fig. S5 – Fig. S6 [**Supplementary Information**]). This is in line with previous studies that failed to detect significant diversification shifts either across Annonaceae as a whole or for subfamily (Couvreur *et al.*, 2011a; Erkens *et al.*, 2012) or within the Annonoideae subfamily (which inlcudes Monodoreae) (Massoni *et al.*, 2015a), suggesting a rather constant rate of diversification at least at higher taxonomic levels in Annonaceae. Nevertheless, diversification rates in Monodoreae are not homogeneous across genera (Fig. 5, Fig. S3 – Fig. S4 [**Supplementary Information**]), and BAMM has been shown in some cases not to detect shifts even though they exist (Rabosky, 2014; Mitchell *et al.*, 2019). All analyses found higher diversification rates in the genus *Uvariopsis* when compared to the other genera. With 20 species (17 described and 3 undescribed, see Dagallier *et al.*, in press), *Uvariopsis* is one of the most species-rich and youngest genera of the tribe (crown node: median 5.90 Ma, 95% HPD 5.21–6.57 Ma). Using the methods of moments (Magallón and Sanderson, 2001), that is using species richness and age of the stem node, *Uvariopsis* was identified as one of the fastest diversifying Annonaceae genera under a no extinction hypothesis (Couvreur *et al.*, 2011a). Indeed, all extant species diverged between ca. 4.5 and 1 Ma, whereas most of the species in the other rich genera (*Isolona* (20 species), *Monodora* (14 species), *Uvariodendron* (18 species)) diverged between 10 and 4 Ma (Fig. 2). Morphologically, *Uvariopsis* has several features differentiating it from other Monodoreae. All but one species are monoecious, i.e. have separated male (staminate) and female (pistillate) flowers on the same individual (except *U. bisexualis*, not included in this study) and they all present a reduction of the perianth parts (2 sepals and 3 or 4 petals) when compared to the typical Annonaceae flower (3 sepals and 6 petals) (Dagallier, 2021; Dagallier

et al., in press). Such association between monoecy and reduction of perianth parts has been suggested to be an optimization of resources allocation to sex (Jong *et al.*, 2008). Monoecy could be evolutionary advantageous to avoid self-pollination (Pang *et al.*, 2013), but the flowers of most Annonaceae species generally avoid self-pollination with temporal variation of the stamens and carpels maturation (Pang and Saunders, 2014). Another evolutionary advantage of monoecy is likely conferred by the flexibility in resource allocation to male and female functions (Bertin, 1993). However, recent analyses found unisexual flowers associated with lower diversification rates than in bisexual flowers and androdioecous flowers at the population level (Xue *et al.*, 2020). Three species of *Uvariopsis* are pollinated by Diptera (Gottsberger *et al.*, 2011; Mertens *et al.*, 2018), which is quite uncommon in Annonaceae (Saunders, 2012). Shifts in pollination syndromes have been suggested to be responsible for shifts in diversification (Valente *et al.*, 2012; Breitkopf *et al.*, 2015; Lagomarsino *et al.*, 2016; Serrano-Serrano *et al.*, 2017). One would be tempted to relate the peculiarities of *Uvariopsis* (monoecy and Diptera pollination) to its higher diversification rates relatively to the other Monodoreae genera. However, given these characters appeared only once in Monodoreae, testing for their influence on diversification rates (e.g. with SSE models; Maddison *et al.*, 2007) could provide spurious inferences (Maddison and FitzJohn, 2015).

Conclusion

Our study brings new and more detailed insights into the evolution of TRF in Africa during the Cenozoic. By focusing on Monodoreae, we found that this clade originated in East African TRF during the late Oligocene (*ca.* 25 Ma) after the Eocene–Oligocene Transition and expanded toward Central/West Africa during the early to middle Miocene, supporting the existence of a pan-African rain forest until *ca.* 13.5 Ma. There is no evidence for clear discrete

and synchronous vicariance events between forests blocks during the middle Miocene as previously suggested, but instead range contractions that led to speciation and supporting the hypothesis of TRF fragmentation due to aridification in Africa. However, we also inferred clades spanning several forest blocks during the middle Miocene, suggesting that the TRF blocks were more connected than previously thought. The Monodoreae likely experienced sudden extinction during the late Miocene, supporting the drastic reduction of the TRF linked to aridification. This was quikcly followed by high speciation rates, suggesting that both the fragmentation and the following re-connection of the TRF in the early Pliocene stimulated diversification. Such a high diversification was likely associated with the increasing African paleo-elevation during the late Miocene and Pliocene, supporting the idea that the uplift of East Africa was a factor that promoted diversification.

Funding

This work was supported by the Agence Nationale de la Recherche (AFRODYN Grant Number: ANR-15-CE02-0002-01) and the European Research Council under the European Union's Horizon 2020 research and innovation program (grant agreement No. 865787) both to TLPC.

Supplementary Information description

Fig. S1. Phylogenetic inference of the Monodoreae and outgroups (other Annonaceae + *Eupomatia*)

Fig. S2. Extinction rates of Monodoreae estimated using ClaDS

Fig. S3. Speciation, extinction diversification of Monodoreae estimated using RevBayes (BSDR model)

Fig. S5. Traces of the MCMC run for the BAMM analysis

Fig. S6. Posterior probabilities of the number of diversification rates shifts in the Monodoreae phylogeny according to BAMM.

Fig. S7 – S16. Results of the CoMET analysis, with different prior on the chance of survival to a mass extinction event (5 – 50%).

Fig. S17. Estimated proportion of C4 plants in tropical Africa interpolated from Polissar et al. 2019

Table S1. Information on the vouchers used in this study.

Table S2. Length and best substitution model of the 32 loci used in this study.

Acknowledgements

We thank Lars Chatrou, Susanne Renner, Muthama Muasya, Sidonie Bellot, Myriam Gaudeul, and Gael Kergoat for the discussion on an earlier version of this manuscript. The authors acknowledge the ISO 9001 certified IRD i-Trop HPC (member of the South Green Platform) at IRD Montpellier for providing HPC resources that have contributed to the research results reported within this paper. URL: https://bioinfo.ird.fr/-http://www.southgreen.fr

Literature cited

Aduse-Poku K, van Bergen E, Sáfián S, *et al.* 2021. Miocene climate and habitat change drove diversification in *Bicyclus*, Africa's largest radiation of satyrine butterflies. *Systematic Biology* **71**: 570–88.

Ali JR, Huber M. **2010**. Mammalian biodiversity on Madagascar controlled by ocean currents. *Nature* **463**: 653–6.

Ali JR, Hedges SB. **2022**. A review of geological evidence bearing on proposed Cenozoic land connections between Madagascar and Africa and its relevance to biogeography. *Earth-Science Reviews* **232**: 104103.

Antonelli A, Kissling WD, Flantua SGA, *et al.* 2018. Geological and climatic influences on mountain biodiversity. *Nature Geoscience* **11**: 718–25.

Antonelli A, Smith RJ, Perrigo AL, *et al.* 2022. Madagascar's extraordinary biodiversity: Evolution, distribution, and use. *Science* **378**: eabf0869.

Armstrong KE, Stone GN, Nicholls JA, *et al.* 2014. Patterns of diversification amongst tropical regions compared: a case study in Sapotaceae. *Frontiers in Genetics* **5**: 362.

Baker WJ, Couvreur TLP. **2013**. Global biogeography and diversification of palms sheds light on the evolution of tropical lineages. I. Historical biogeography. *Journal of Biogeography* **40**: 274–85.

Bankevich A, Nurk S, Antipov D, *et al.* 2012. SPAdes: a new genome assembly algorithm and its applications to single-cell sequencing. *Journal of Computational Biology* **19**: 455–77.

Bell RC, Parra JL, Badjedjea G, *et al.* 2017. Idiosyncratic responses to climate-driven forest fragmentation and marine incursions in reed frogs from Central Africa and the Gulf of Guinea Islands. *Molecular Ecology* **26**: 5223–44.

Bertin RI. **1993**. Incidence of monoecy and dichogamy in relation to self-fertilization in angiosperms. *American Journal of Botany* **80**: 557–60.

Bivand R, Rundel C, Pebesma E, *et al.* 2020. rgeos: Interface to Geometry Engine - Open Source ('GEOS').

826 **Bonnefille R**. **2010**. Cenozoic vegetation, climate changes and hominid evolution in tropical
827 Africa. *Global and Planetary Change* **72**: 390–411.
828 **Boschman LM, Condamine FL**. **2022**. Mountain radiations are not only rapid and recent:
829 Ancient diversification of South American frog and lizard families related to
830 Paleogene Andean orogeny and Cenozoic climate variations. *Global and Planetary*
831 *Change* **208**: 103704.
832 **Botermans M, Sosef MSM, Chatrou LW, Couvreur TLP**. **2011**. Revision of the African
833 genus *Hexalobus* (Annonaceae). *Systematic Botany* **36**: 33–48.
834 **Bouchenak-Khelladi Y, Maurin O, Hurter J, van der Bank M**. **2010**. The evolutionary
835 history and biogeography of Mimosoideae (Leguminosae): An emphasis on African
836 acacias. *Molecular Phylogenetics and Evolution* **57**: 495–508.
837 **Bouckaert R, Vaughan TG, Barido-Sottani J, *et al.* 2019**. BEAST 2.5: An advanced
838 software platform for Bayesian evolutionary analysis. *PLOS Computational Biology*
839 **15**: e1006650.
840 **Brée B, Helmstetter AJ, Bethune K, Ghogue J-P, Sonké B, Couvreur TLP**. **2020**.
841 Diversification of African rainforest restricted clades: Piptostigmateae and Annickieae
842 (Annonaceae). *Diversity* **12**: 227.
843 **Breitkopf H, Onstein RE, Cafasso D, Schlüter PM, Cozzolino S**. **2015**. Multiple shifts to
844 different pollinators fuelled rapid diversification in sexually deceptive *Ophrys* orchids.
845 *New Phytologist* **207**: 377–89.
846 **Brown JW, Walker JF, Smith SA**. **2017**. Phyx: phylogenetic tools for unix. *Bioinformatics*
847 **33**: 1886–8.
848 **Bryja J, Šumbera R, Peterhans JCK, *et al.* 2017**. Evolutionary history of the thicket rats
849 (genus *Grammomys*) mirrors the evolution of African forests since late Miocene.
850 *Journal of Biogeography* **44**: 182–94.

Buerki S, Devey DS, Callmander MW, Phillipson PB, Forest F. **2013**. Spatio-temporal history of the endemic genera of Madagascar. *Botanical Journal of the Linnean Society* **171**: 304–29.

Burgess ND, Butynski TM, Cordeiro NJ, *et al.* 2007. The biological importance of the Eastern Arc Mountains of Tanzania and Kenya. *Biological Conservation* **134**: 209–31.

Chatrou LW, Pirie MD, Erkens RHJ, *et al.* 2012. A new subfamilial and tribal classification of the pantropical flowering plant family Annonaceae informed by molecular phylogenetics. *Botanical Journal of the Linnean Society* **169**: 5–40.

Cheek M, Luke WRQ, Gosline G. **2022**. *Lukea* gen. nov. (Monodoreae-Annonaceae) with two new threatened species of shrub from the forests of the Udzungwas, Tanzania and Kaya Ribe, Kenya. *Kew Bulletin* **77**: 647–64.

Chen J, Thomas DC, Saunders RMK. **2019**. Geographic range and habitat reconstructions shed light on palaeotropical intercontinental disjunction and regional diversification patterns in *Artabotrys* (Annonaceae). *Journal of Biogeography* **46**: 2690–705.

Chorowicz J. **2005**. The East African rift system. *Journal of African Earth Sciences* **43**: 379–410.

Condamine FL, Rolland J, Morlon H. **2013**. Macroevolutionary perspectives to environmental change. *Ecology Letters* **16**: 72–85.

Condamine FL, Rolland J, Höhna S, Sperling FAH, Sanmartín I. **2018**. Testing the role of the Red Queen and Court Jester as drivers of the macroevolution of Apollo butterflies Wiegmann B (ed). *Systematic Biology* **67**: 940–64.

Couvreur TLP, Gereau RE, Wieringa JJ, Richardson JE. **2006**. Description of four new species of *Monodora* and *Isolona* (Annonaceae) from Tanzania and an overview of Tanzanian Annonaceae diversity. *Adansonia* **28**: 243–66.

Couvreur TLP, Chatrou LW, Sosef MSM, Richardson JE. **2008**. Molecular phylogenetics reveal multiple Tertiary vicariance origins of the African rain forest trees. *BMC Biology* **6**: 54.

Couvreur TLP. **2009**. Monograph of the syncarpous African genera *Isolona* and *Monodora* (Annonaceae). *Systematic Botany Monographs* **87**: 1–150.

Couvreur TLP, Pirie MD, Chatrou LW, *et al.* 2011a. Early evolutionary history of the flowering plant family Annonaceae: steady diversification and boreotropical geodispersal. *Journal of Biogeography* **38**: 664–80.

Couvreur TLP, Porter-Morgan H, Wieringa JJ, Chatrou LW. **2011b**. Little ecological divergence associated with speciation in two African rain forest tree genera. *BMC Evolutionary Biology* **11**: 296.

Couvreur TLP. **2014**. Revision of the African genus *Uvariastrum* (Annonaceae). *PhytoKeys* **33**: 1–40.

Couvreur TLP. **2015**. Odd man out: why are there fewer plant species in African rain forests? *Plant Systematics and Evolution* **301**: 1299–313.

Couvreur TLP, Helmstetter AJ, Koenen EJM, *et al.* 2019. Phylogenomics of the major tropical plant family Annonaceae using targeted enrichment of nuclear genes. *Frontiers in Plant Science* **9**.

Couvreur TLP, Dauby G, Blach-Overgaard A, *et al.* 2021. Tectonics, climate and the diversification of the tropical African terrestrial flora and fauna. *Biological Reviews* **96**: 16–51.

Currano ED, Jacobs BF, Pan AD, Tabor NJ. **2011**. Inferring ecological disturbance in the fossil record: A case study from the late Oligocene of Ethiopia. *Palaeogeography, Palaeoclimatology, Palaeoecology* **309**: 242–52.

Currano ED, Jacobs BF, Pan AD. **2021**. Is Africa really an “odd man out”? Evidence for diversity decline across the Oligocene-Miocene boundary. *International Journal of Plant Sciences* **182**: 551–63.

Dagallier L-PMJ, Janssens SB, Dauby G, *et al.* 2020. Cradles and museums of generic plant diversity across tropical Africa. *New Phytologist* **225**: 2196–213.

Dagallier L-PMJ. **2021**. Diversification of the tropical African flora: spatial and temporal approaches. Thesis, University of Montpellier, France.

Dagallier L-PMJ, Mbago FM, Couderc M, *et al.* in press. Phylogenomic inference of the African tribe Monodoreae (Annonaceae) and taxonomic revision of *Dennettia*, *Uvariodendron* and *Uvariopsis*. *PhytoKeys*.

Darriba D, Posada D, Kozlov AM, Stamatakis A, Morel B, Flouri T. **2020**. ModelTest-NG: a new and scalable tool for the selection of dna and protein evolutionary models. *Molecular Biology and Evolution* **37**: 291–4.

Dauby G, Zaiss R, Overgaard A-B, *et al.* 2016. RAINBIO: a mega-database of tropical African vascular plants distributions. *PhytoKeys* **74**: 1–18.

Davis CC, Bell CD, Fritsch PW, Mathews S. **2002**. Phylogeny of *Acridocarpus-Brachylophon* (Malpighiaceae): Implications for Tertiary tropical floras and Afroasian biogeography. *Evolution* **56**: 2395–405.

Demenou BB, Doucet J-L, Hardy OJ. **2018**. History of the fragmentation of the African rain forest in the Dahomey Gap: insight from the demographic history of Terminalia *superba*. *Heredity* **120**: 547.

Demenou BB, Migliore J, Heuertz M, *et al.* 2020. Plastome phylogeography in two African rain forest legume trees reveals that Dahomey Gap populations originate from the Cameroon volcanic line. *Molecular Phylogenetics and Evolution* **150**: 106854.

Demos TC, Kerbis Peterhans JC, Agwanda B, Hickerson MJ. **2014**. Uncovering cryptic diversity and refugial persistence among small mammal lineages across the Eastern Afromontane biodiversity hotspot. *Molecular Phylogenetics and Evolution* **71**: 41–54.

Dimitrov D, Nogués-Bravo D, Scharff N. **2012**. Why do tropical mountains support exceptionally high biodiversity? The Eastern Arc Mountains and the drivers of *Saintpaulia* diversity. *PLOS ONE* **7**: e48908.

Droissart V, Dauby G, Hardy OJ, *et al.* 2018. Beyond trees: Biogeographical regionalization of tropical Africa. *Journal of Biogeography* **45**: 1153–67.

Drummond AJ, Ho SYW, Phillips MJ, Rambaut A. **2006**. Relaxed phylogenetics and dating with confidence. *PLOS Biology* **4**: e88.

Duminil J, Mona S, Mardulyn P, *et al.* 2015. Late Pleistocene molecular dating of past population fragmentation and demographic changes in African rain forest tree species supports the forest refuge hypothesis. *Journal of Biogeography* **42**: 1443–54.

Eiserhardt WL, Couvreur TLP, Baker WJ. **2017**. Plant phylogeny as a window on the evolution of hyperdiversity in the tropical rainforest biome. *New Phytologist* **214**: 1408–22.

Erkens RHJ, Chatrou LW, Couvreur TLP. **2012**. Radiations and key innovations in an early branching angiosperm lineage (Annonaceae; Magnoliales). *Botanical Journal of the Linnean Society* **169**: 117–34.

Faye A, Pintaud J-C, Baker WJ, Vigouroux Y, Sonke B, Couvreur TLP. **2016**. Phylogenetics and diversification history of African rattans (Calamoideae, Ancistrophyllinae). *Botanical Journal of the Linnean Society* **182**: 256–71.

Fer I, Tietjen B, Jeltsch F, Trauth MH. **2017**. Modelling vegetation change during Late Cenozoic uplift of the East African plateaus. *Palaeogeography, Palaeoclimatology, Palaeoecology* **467**: 120–30.

948 **Finch J, Leng MJ, Marchant R**. **2009**. Late Quaternary vegetation dynamics in a
949 biodiversity hotspot, the Uluguru Mountains of Tanzania. *Quaternary Research* **72**:
950 111–22.
951 **Fjeldså J, Lovett JC**. **1997**. Geographical patterns of old and young species in African forest
952 biota: the significance of specific montane areas as evolutionary centres. *Biodiversity*
953 *& Conservation* **6**: 325–46.
954 **Fjeldså J, Johansson US, Lokugalappatti LGS, Bowie RCK**. **2007**. Diversification of
955 African greenbuls in space and time: linking ecological and historical processes.
956 *Journal of Ornithology* **148**: 359–67.
957 **Fjeldså J, Bowie RCK**. **2008**. New perspectives on the origin and diversification of Africa's
958 forest avifauna. *African Journal of Ecology* **46**: 235–47.
959 **Fuchs J, Pons J-M, Bowie RCK**. **2017**. Biogeography and diversification dynamics of the
960 African woodpeckers. *Molecular Phylogenetics and Evolution* **108**: 88–100.
961 **Gautier-Hion A, Duplantier J-M, Quris R, *et al.* 1985**. Fruit characters as a basis of fruit
962 choice and seed dispersal in a tropical forest vertebrate community. *Oecologia* **65**:
963 324–37.
964 **Gentry AH**. **1982**. Neotropical floristic diversity: phytogeographical connections between
965 central and south america, pleistocene climatic flutuations, or an accident of the
966 andean orogeny? *Annals of the Missouri Botanical Garden* **69**.
967 **Gonçalves M, Siegismund HR, Vuuren BJ van, Ferrand N, Godinho R**. **2021**.
968 Evolutionary history of the roan antelope across its African range. *Journal of*
969 *Biogeography* **n/a**.
970 **Gottsberger G, Meinke S, Porembski S**. **2011**. First records of flower biology and
971 pollination in African Annonaceae: *Isolona*, *Piptostigma*, *Uvariodendron*, *Monodora*

and *Uvariopsis*. *Flora - Morphology, Distribution, Functional Ecology of Plants* **206**: 498–510.

Griffiths CJ. **1993**. The geological evolution of East Africa. In: Lovett JC, Wasser SK (eds). *Biogeography and Ecology of the Rain Forests of Eastern Africa*. Cambridge University Press: Cambridge, 9–22.

Guillocheau F, Simon B, Baby G, Bessin P, Robin C, Dauteuil O. **2018**. Planation surfaces as a record of mantle dynamics: The case example of Africa. *Gondwana Research* **53**: 82–98.

Haywood AM, Hill DJ, Dolan AM, *et al.* 2013. Large-scale features of Pliocene climate: results from the Pliocene Model Intercomparison Project. *Climate of the Past* **9**: 191–209.

Helmstetter AJ, Béthune K, Kamdem NG, Sonké B, Couvreur TLP. **2020**. Individualistic evolutionary responses of Central African rain forest plants to Pleistocene climatic fluctuations. *Proceedings of the National Academy of Sciences* **117**: 32509–18.

Herbert TD, Lawrence KT, Tzanova A, Peterson LC, Caballero-Gill R, Kelly CS. **2016**. Late Miocene global cooling and the rise of modern ecosystems. *Nature Geoscience* **9**: 843–7.

Höhna S, May MR, Moore BR. **2015**. Phylogeny simulation and diversification rate analysis with TESS.

Höhna S, May MR, Moore BR. **2016**. TESS: an R package for efficiently simulating phylogenetic trees and performing Bayesian inference of lineage diversification rates. *Bioinformatics* **32**: 789–91.

Höhna S, Freyman WA, Nolen Z, Huelsenbeck JP, May MR, Moore BR. **2019**. A Bayesian approach for estimating branch-specific speciation and extinction rates

996 **Holstein N, Renner SS**. **2011**. A dated phylogeny and collection records reveal repeated
997 biome shifts in the African genus *Coccinia* (Cucurbitaceae). *BMC Evolutionary*
998 *Biology* **11**: 28.
999 **Hoorn C, Wesselingh FP, Steege H ter, *et al.* 2010**. Amazonia Through Time: Andean Uplift,
1000 Climate Change, Landscape Evolution, and Biodiversity. *Science* **330**: 927–31.
1001 **Huntley JW, Voelker G**. **2016**. Cryptic diversity in Afro-tropical lowland forests: The
1002 systematics and biogeography of the avian genus *Bleda*. *Molecular Phylogenetics and*
1003 *Evolution* **99**: 297–308.
1004 **Huntley JW, Harvey JA, Pavia M, Boano G, Voelker G**. **2018**. The systematics and
1005 biogeography of the Bearded Greenbuls (Aves: *Criniger*) reveals the impact of Plio-
1006 Pleistocene forest fragmentation on Afro-tropical avian diversity. *Zoological Journal*
1007 *of the Linnean Society* **183**: 672–86.
1008 **Jacobs BF**. **2004**. Palaeobotanical studies from tropical Africa: relevance to the evolution of
1009 forest, woodland and savannah biomes. *Philosophical Transactions of the Royal*
1010 *Society B: Biological Sciences* **359**: 1573–83.
1011 **Jacobs BF, Tabor N, Feseha M, *et al.* 2005**. Oligocene terrestrial strata of northwestern
1012 Ethiopia : a preliminary report on paleoenvironments and paleontology.
1013 *Palaeontologia electronica [electronic resource]. Vol. 8, no. 1 (2005): 19 p.*
1014 **Jacobs BF, Pan AD, Scotese CR**. **2010**. A review of the Cenozoic vegetation history of
1015 Africa. In: *Cenozoic Mammals of Africa*. University of California Press: Berkeley, 57–
1016 72.
1017 **Johnson MG, Gardner EM, Liu Y, *et al.* 2016**. HybPiper: Extracting coding sequence and
1018 introns for phylogenetics from high-throughput sequencing reads using target
1019 enrichment. *Applications in Plant Sciences* **4**: 1600016.

Jong TJ de, Shmida A, Thuijsman F. **2008**. Sex allocation in plants and the evolution of monoecy. *Evolutionary Ecology Research* **10**: 1087–109.

Joordens JCA, Feibel CS, Vonhof HB, Schulp AS, Kroon D. **2019**. Relevance of the eastern African coastal forest for early hominin biogeography. *Journal of Human Evolution* **131**: 176–202.

Kass RE, Raftery AE. **1995**. Bayes Factors. *Journal of the American Statistical Association* **90**: 773–95.

Katoh K, Standley DM. **2013**. MAFFT multiple sequence alignment software version 7: improvements in performance and usability. *Molecular Biology and Evolution* **30**: 772–80.

Kergoat GJ, Condamine FL, Toussaint EFA, *et al.* 2018. Opposite macroevolutionary responses to environmental changes in grasses and insects during the Neogene grassland expansion. *Nature Communications* **9**: 5089.

Kissling WD, Eiserhardt WL, Baker WJ, *et al.* 2012. Cenozoic imprints on the phylogenetic structure of palm species assemblages worldwide. *Proceedings of the National Academy of Sciences* **109**: 7379–84.

Kocsis AT, Raja NB. **2021**. chronosphere: Earth System History Variables.

Lagomarsino LP, Condamine FL, Antonelli A, Mulch A, Davis CC. **2016**. The abiotic and biotic drivers of rapid diversification in Andean bellflowers (Campanulaceae). *New Phytologist* **210**: 1430–42.

Leaché AD, Portik DM, Rivera D, *et al.* 2019. Exploring rain forest diversification using demographic model testing in the African foam-nest treefrog *Chiromantis rufescens*. *Journal of Biogeography* **46**: 2706–21.

Lehmann CER, Archibald SA, Hoffmann WA, Bond WJ. **2011**. Deciphering the distribution of the savanna biome. *New Phytologist* **191**: 197–209.

Li H, Durbin R. **2009**. Fast and accurate short read alignment with Burrows-Wheeler transform. *Bioinformatics (Oxford, England)* **25**: 1754–60.

Linder HP. **2017**. East African Cenozoic vegetation history. *Evolutionary Anthropology: Issues, News, and Reviews* **26**: 300–12.

Lischer HEL, Excoffier L. **2012**. PGDSpider: an automated data conversion tool for connecting population genetics and genomics programs. *Bioinformatics* **28**: 298–9.

Loader SP, Pisani D, Cotton JA, Gower DJ, Day JJ, Wilkinson M. **2007**. Relative time scales reveal multiple origins of parallel disjunct distributions of African caecilian amphibians. *Biology Letters* **3**: 505–8.

Loader SP, Ceccarelli FS, Menegon M, *et al.* 2014. Persistence and stability of Eastern Afromontane forests: evidence from brevicipitid frogs. *Journal of Biogeography* **41**: 1781–92.

Lompo D, Vinceti B, Konrad H, Gaisberger H, Geburek T. **2018**. Phylogeography of African locust bean (*Parkia biglobosa*) reveals genetic divergence and spatially structured populations in West and Central Africa. *Journal of Heredity* **109**: 811–24.

Lovett JC, Marchant R, Taplin J, Küper W. **2005**. The oldest rainforests in Africa: Stability or resilience for survival and diversity? In: Purvis A, Gittleman JL, Brooks T (eds). *Phylogeny and Conservation*. Cambridge University Press. Cambridge University Press: Cambridge, 198–229.

Macgregor D. **2015**. History of the development of the East African Rift System: A series of interpreted maps through time. *Journal of African Earth Sciences* **101**: 232–52.

Maddison WP, Midford PE, Otto SP. **2007**. Estimating a binary character's effect on speciation and extinction. *Systematic Biology* **56**: 701–10.

Maddison WP, FitzJohn RG. **2015**. The unsolved challenge to phylogenetic correlation tests for categorical characters. *Systematic Biology* **64**: 127–36.

Magallón S, Sanderson MJ. **2001**. Absolute diversification rates in angiosperm clades. *Evolution* **55**: 1762–80.

Malhi Y, Gardner TA, Goldsmith GR, Silman MR, Zelazowski P. **2014**. Tropical forests in the Anthropocene. *Annual Review of Environment and Resources* **39**: 125–59.

Maliet O, Hartig F, Morlon H. **2019**. A model with many small shifts for estimating species-specific diversification rates. *Nature Ecology & Evolution* **3**: 1086–92.

Maliet O, Morlon H. **2021**. Fast and accurate estimation of species-specific diversification rates using data augmentation. *Systematic Biology*: 14.

Massoni J, Couvreur TLP, Sauquet H. **2015a**. Five major shifts of diversification through the long evolutionary history of Magnoliidae (Angiosperms). *BMC Evolutionary Biology* **15**: 49.

Massoni J, Doyle J, Sauquet H. **2015b**. Fossil calibration of Magnoliidae, an ancient lineage of Angiosperms. *Palaeontologia Electronica* **18**: 1–25.

Masters JC, Génin F, Zhang Y, *et al.* 2021. Biogeographic mechanisms involved in the colonization of Madagascar by African vertebrates: Rifting, rafting and runways. *Journal of Biogeography* **48**: 492–510.

Matzke NJ. **2014**. Model selection in historical biogeography reveals that founder-event speciation is a crucial process in island clades. *Systematic Biology* **63**: 951–70.

May MR, Höhna S, Moore BR. **2016**. A Bayesian approach for detecting the impact of mass-extinction events on molecular phylogenies when rates of lineage diversification may vary. *Methods in Ecology and Evolution* **7**: 947–59.

Mayaux P, Bartholomé E, Fritz S, Belward A. **2004**. A new land-cover map of Africa for the year 2000. *Journal of Biogeography* **31**: 861–77.

Menegon M, Loader SP, Marsden SJ, Branch WR, Davenport TRB, Ursenbacher S. **2014**. The genus *Atheris* (Serpentes: Viperidae) in East Africa: Phylogeny and the role

of rifting and climate in shaping the current pattern of species diversity. *Molecular Phylogenetics and Evolution* **79**: 12–22.

Mertens JEJ, Tropek R, Dzekashu FF, Maicher V, Fokam EB, Janeček Š. **2018**. Communities of flower visitors of *Uvariopsis dioica* (Annonaceae) in lowland forests of Mt. Cameroon, with notes on its potential pollinators. *African Journal of Ecology* **56**: 146–52.

Mitchell JS, Etienne RS, Rabosky DL. **2019**. Inferring diversification rate variation from phylogenies with fossils. *Systematic Biology* **68**: 1–18.

Moritz C, Patton JL, Schneider CJ, Smith TB. **2000**. Diversification of rainforest faunas: an integrated molecular approach. *Annual Review of Ecology and Systematics* **31**: 533–63.

Morley RJ, Richards K. **1993**. Gramineae cuticle: a key indicator of Late Cenozoic climatic change in the Niger Delta. *Review of Palaeobotany and Palynology* **77**: 119–27.

Morley RJ. **2000**. *Origin and evolution of tropical rain forests*. John Wiley & Sons Ltd.: Chichester, England.

Morley RJ. **2011**. Cretaceous and Tertiary climate change and the past distribution of megathermal rainforests. In: Bush M, Flenley J, Gosling W (eds). *Tropical Rainforest Responses to Climatic Change*. Springer: Berlin, Heidelberg, 1–34.

Muellner-Riehl AN. **2019**. Mountains as evolutionary arenas: Patterns, emerging approaches, paradigm shifts, and their implications for plant phylogeographic research in the Tibeto-Himalayan region. *Frontiers in Plant Science* **10**: 195.

Nicolas V, Fabre P-H, Bryja J, *et al.* 2020. The phylogeny of the African wood mice (Muridae, *Hylomyscus*) based on complete mitochondrial genomes and five nuclear genes reveals their evolutionary history and undescribed diversity. *Molecular Phylogenetics and Evolution* **144**: 106703.

Nkonmeneck WPT, Allen KE, Hime PM, *et al.* 2022. Diversification and historical demography of *Rhampholeon* spectrum in West-Central Africa. *PLOS ONE* **17**: e0277107.

Olson DM, Dinerstein E, Wikramanayake ED, *et al.* 2001. Terrestrial Ecoregions of the World: A New Map of Life on Earth. *BioScience* **51**: 933.

Onstein RE, Baker WJ, Couvreur TLP, *et al.* 2018. To adapt or go extinct? The fate of megafaunal palm fruits under past global change. *Proceedings of the Royal Society B: Biological Sciences* **285**: 20180882.

Onstein RE, Kissling WD, Chatrou LW, Couvreur TLP, Morlon H, Sauquet H. **2019**. Which frugivory-related traits facilitated historical long-distance dispersal in the custard apple family (Annonaceae)? *Journal of Biogeography* **46**: 1874–88.

Palazzesi L, Hidalgo O, Barreda VD, Forest F, Höhna S. **2022**. The rise of grasslands is linked to atmospheric CO2 decline in the late Palaeogene. *Nature Communications* **13**: 293.

Pan AD, Jacobs BF, Dransfield J, Baker WJ. **2006**. The fossil history of palms (Arecaceae) in Africa and new records from the Late Oligocene (28–27 Mya) of north-western Ethiopia. *Botanical Journal of the Linnean Society* **151**: 69–81.

Pan AD. **2010**. Rutaceae leaf fossils from the Late Oligocene (27.23Ma) Guang River flora of northwestern Ethiopia. *Review of Palaeobotany and Palynology* **159**: 188–94.

Pang C-C, Scharaschkin T, Su YCF, Saunders RMK. **2013**. Functional monoecy due to delayed anther dehiscence: A novel mechanism in *Pseuduvaria mulgraveana* (Annonaceae). *PLOS ONE* **8**: e59951.

Pang C-C, Saunders RMK. **2014**. The evolution of alternative mechanisms that promote outcrossing in Annonaceae, a self-compatible family of early-divergent angiosperms. *Botanical Journal of the Linnean Society* **174**: 93–109.

Parmentier I, Malhi Y, Senterre B, *et al.* 2007. The odd man out? Might climate explain the lower tree α-diversity of African rain forests relative to Amazonian rain forests? *Journal of Ecology* **95**: 1058–71.

Pebesma E, Bivand R, Rowlingson B, *et al.* 2021. sp: Classes and Methods for Spatial Data.

Pirie MD, Doyle JA. **2012**. Dating clades with fossils and molecules: the case of Annonaceae. *Botanical Journal of the Linnean Society* **169**: 84–116.

Plana V. **2004**. Mechanisms and tempo of evolution in the African Guineo-Congolian rainforest. *Philosophical Transactions of the Royal Society B: Biological Sciences* **359**: 1585–94.

Plummer M, Best N, Cowles K, *et al.* 2020. coda: Output analysis and diagnostics for MCMC.

Pokorny L, Riina R, Mairal M, *et al.* 2015. Living on the edge: timing of Rand Flora disjunctions congruent with ongoing aridification in Africa. *Frontiers in Genetics* **6**: 154.

Polissar PJ, Rose C, Uno KT, Phelps SR, deMenocal P. **2019**. Synchronous rise of African C4 ecosystems 10 million years ago in the absence of aridification. *Nature Geoscience* **12**: 657–60.

Rabinowitz PD, Woods S. **2006**. The Africa–Madagascar connection and mammalian migrations. *Journal of African Earth Sciences* **44**: 270–6.

Rabosky DL. **2014**. Automatic detection of key innovations, rate shifts, and diversity-dependence on phylogenetic trees. *PLOS ONE* **9**: e89543.

Rabosky DL, Grundler M, Anderson C, *et al.* 2014. BAMMtools: an R package for the analysis of evolutionary dynamics on phylogenetic trees Kembel S (ed). *Methods in Ecology and Evolution* **5**: 701–7.

Rahbek C, Borregaard MK, Colwell RK, *et al.* 2019. Humboldt's enigma: What causes global patterns of mountain biodiversity? *Science* **365**: 1108–13.

Rambaut A, Drummond AJ, Xie D, Baele G, Suchard MA. **2018**. Posterior summarization in bayesian phylogenetics using Tracer 1.7. *Systematic Biology* **67**: 901–4.

Ree RH, Smith SA. **2008**. Maximum likelihood inference of geographic range evolution by dispersal, local extinction, and cladogenesis. *Systematic Biology* **57**: 4–14.

Ree RH, Sanmartín I. **2018**. Conceptual and statistical problems with the DEC+J model of founder-event speciation and its comparison with DEC via model selection. *Journal of Biogeography* **45**: 741–9.

Remis MJ, Dierenfeld ES, Mowry CB, Carroll RW. **2001**. Nutritional aspects of western lowland gorilla (*Gorilla gorilla gorilla*) diet during seasons of fruit scarcity at Bai Hokou, Central African Republic. *International Journal of Primatology* **22**: 807–36.

Renner SS. **2004**. Multiple Miocene Melastomataceae dispersal between Madagascar, Africa and India Pennington PT, Cronk QCB, Richardson JA (eds). *Philosophical Transactions of the Royal Society of London. Series B: Biological Sciences* **359**: 1485–94.

Retallack GJ, Dugas DP, Bestland EA. **1990**. Fossil soils and grasses of a Middle Miocene East African grassland. *Science* **247**: 1325–8.

Ring U, Albrecht C, Schrenk F. **2018**. The east African rift system: tectonics, climate and biodiversity. In: *Mountains, Climate and Biodiversity*. John Wiley & Sons, 391–406.

Ripley S original by JRR port by B. **2017**. pspline: Penalized smoothing splines.

Rogers ME, Abernethy K, Bermejo M, *et al.* 2004. Western gorilla diet: A synthesis from six sites. *American Journal of Primatology* **64**: 173–92.

Salzmann U, Hoelzmann P. **2005**. The Dahomey Gap: an abrupt climatically induced rain forest fragmentation in West Africa during the late Holocene. *The Holocene* **15**: 190–9.

Saunders RMK. **2012**. The diversity and evolution of pollination systems in Annonaceae. *Botanical Journal of the Linnean Society* **169**: 222–44.

Sauquet H, DOYLE JA, SCHARASCHKIN T, *et al.* 2003. Phylogenetic analysis of Magnoliales and Myristicaceae based on multiple data sets: implications for character evolution. *Botanical Journal of the Linnean Society* **142**: 125–86.

Scotese CR, Wright N. **2018**. PALEOMAP Paleodigital Elevation Models (PaleoDEMS) for the Phanerozoic. PALEOMAP Project.

Ségalen L, Lee-Thorp JA, Cerling T. **2007**. Timing of C4 grass expansion across sub-Saharan Africa. *Journal of Human Evolution* **53**: 549–59.

Senut B, Pickford M, Ségalen L. **2009**. Neogene desertification of Africa. *Comptes Rendus Geoscience* **341**: 591–602.

Sepulchre P, Ramstein G, Fluteau F, Schuster M, Tiercelin J-J, Brunet M. **2006**. Tectonic uplift and eastern Africa aridification. *Science* **313**: 1419–23.

Serrano-Serrano ML, Rolland J, Clark JL, Salamin N, Perret M. **2017**. Hummingbird pollination and the diversification of angiosperms: an old and successful association in Gesneriaceae. *Proceedings of the Royal Society B: Biological Sciences* **284**: 20162816.

van Setten AK, Koek-Noorman J. **1992**. *Fruits and seeds of Annonaceae: morphology and its significance for classification*. Schweizerbart: Stuttgart.

Smith SA, Brown JW, Walker JF. **2018**. So many genes, so little time: A practical approach to divergence-time estimation in the genomic era. *PLOS ONE* **13**: e0197433.

Sommerfeld A, Prömmel K, Cubasch U. **2016**. The East African Rift System and the impact of orographic changes on regional climate and the resulting aridification. *International Journal of Earth Sciences* **105**: 1779–94.

Stamatakis A. **2014**. RAxML version 8: a tool for phylogenetic analysis and post-analysis of large phylogenies. *Bioinformatics* **30**: 1312–3.

Talavera G, Castresana J. **2007**. Improvement of phylogenies after removing divergent and ambiguously aligned blocks from protein sequence alignments. *Systematic Biology* **56**: 564–77.

Thomas DC, Chatrou LW, Stull GW, *et al.* 2015. The historical origins of palaeotropical intercontinental disjunctions in the pantropical flowering plant family Annonaceae. *Perspectives in Plant Ecology, Evolution and Systematics* **17**: 1–16.

Tolley KA, Tilbury CR, Measey GJ, Menegon M, Branch WR, Matthee CA. **2011**. Ancient forest fragmentation or recent radiation? Testing refugial speciation models in chameleons within an African biodiversity hotspot: Palaeoendemic chameleon lineages in East Africa. *Journal of Biogeography* **38**: 1748–60.

Tolley KA, Townsend TM, Vences M. **2013**. Large-scale phylogeny of chameleons suggests African origins and Eocene diversification. *Proceedings of the Royal Society B: Biological Sciences* **280**: 20130184.

Tosso F, Hardy OJ, Doucet J-L, Daïnou K, Kaymak E, Migliore J. **2018**. Evolution in the Amphi-Atlantic tropical genus *Guibourtia* (Fabaceae, Detarioideae), combining NGS phylogeny and morphology. *Molecular Phylogenetics and Evolution* **120**: 83–93.

Tutin CEG, Fernandez M. **1993**. Composition of the diet of chimpanzees and comparisons with that of sympatric lowland gorillas in the lopé reserve, gabon. *American Journal of Primatology* **30**: 195–211.

Uno KT, Polissar PJ, Jackson KE, deMenocal PB. **2016**. Neogene biomarker record of vegetation change in eastern Africa. *Proceedings of the National Academy of Sciences* **113**: 6355–63.

Valente LM, Manning JC, Goldblatt P, Vargas P. **2012**. Did pollination shifts drive diversification in southern African *Gladiolus*? Evaluating the model of pollinator-driven speciation. *The American Naturalist* **180**: 83–98.

Veranso-Libalah MC, Kadereit G, Stone RD, Couvreur TLP. **2018**. Multiple shifts to open habitats in Melastomateae (Melastomataceae) congruent with the increase of African Neogene climatic aridity. *Journal of Biogeography* **45**: 1420–31.

Verdcourt B. **1971**. *Flora of Tropical East Africa: Annonaceae*.

Vincens A, Tiercelin J-J, Buchet G. **2006**. New Oligocene–early Miocene microflora from the southwestern Turkana Basin. *Palaeogeography, Palaeoclimatology, Palaeoecology* **239**: 470–86.

Voelker G, Outlaw RK, Bowie RCK. **2010**. Pliocene forest dynamics as a primary driver of African bird speciation. *Global Ecology and Biogeography* **19**: 111–21.

Vollesen K. **1980**. Notes on Annonaceae from Tanzania. *Botaniska Notiser* **133**: 53–62.

Westerhold T, Marwan N, Drury AJ, *et al.* 2020. An astronomically dated record of Earth's climate and its predictability over the last 66 million years. *Science* **369**: 1383–7.

White LJT, Tutin CEG, Fernandez M. **1993**. Group composition and diet of forest elephants, Loxodonta africana *cyclotis* Matschie 1900, in the Lopé Reserve, Gabon. *African Journal of Ecology* **31**: 181–99.

Wichura H, Jacobs LL, Lin A, *et al.* 2015. A 17-My-old whale constrains onset of uplift and climate change in east Africa. *Proceedings of the National Academy of Sciences* **112**: 3910–5.

Wilson EO. **1988**. *Biodiversity*, National Academy of Sciences/Smithsonian Institution, Division on Earth and Life Studies, Commission on Life Sciences (eds). National Academies Press: Washington D.C.

Xue B, Guo X, Landis JB, *et al.* 2020. Accelerated diversification correlated with functional traits shapes extant diversity of the early divergent angiosperm family Annonaceae. *Molecular Phylogenetics and Evolution* **142**: 106659.

Yao G, Drew BT, Yi T-S, Yan H-F, Yuan Y-M, Ge X-J. **2016**. Phylogenetic relationships, character evolution and biogeographic diversification of *Pogostemon* s.l. (Lamiaceae). *Molecular Phylogenetics and Evolution* **98**: 184–200.

Yoder AD, Nowak MD. **2006**. Has vicariance or dispersal been the predominant biogeographic force in Madagascar? Only time will tell. *Annual Review of Ecology, Evolution, and Systematics* **37**: 405–31.

Zachos JC, Dickens GR, Zeebe RE. **2008**. An early Cenozoic perspective on greenhouse warming and carbon-cycle dynamics. *Nature* **451**: 279–83.

Zhou L, Su YCF, Thomas DC, Saunders RMK. **2012**. 'Out-of-Africa' dispersal of tropical floras during the Miocene climatic optimum: evidence from *Uvaria* (Annonaceae). *Journal of Biogeography* **39**: 322–35.

Figure captions

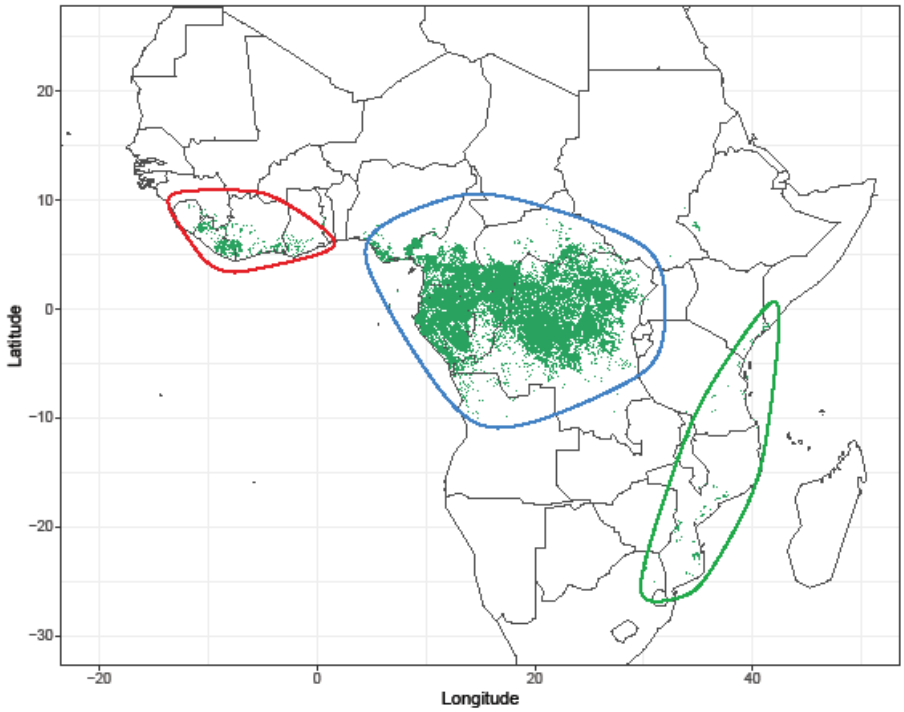

Fig. 1: Map of the tropical rain forest of Africa (after Mayaux *et al.*, 2004): Western block (red), Central block (blue), Eastern block (green) and Madagascar (yellow).

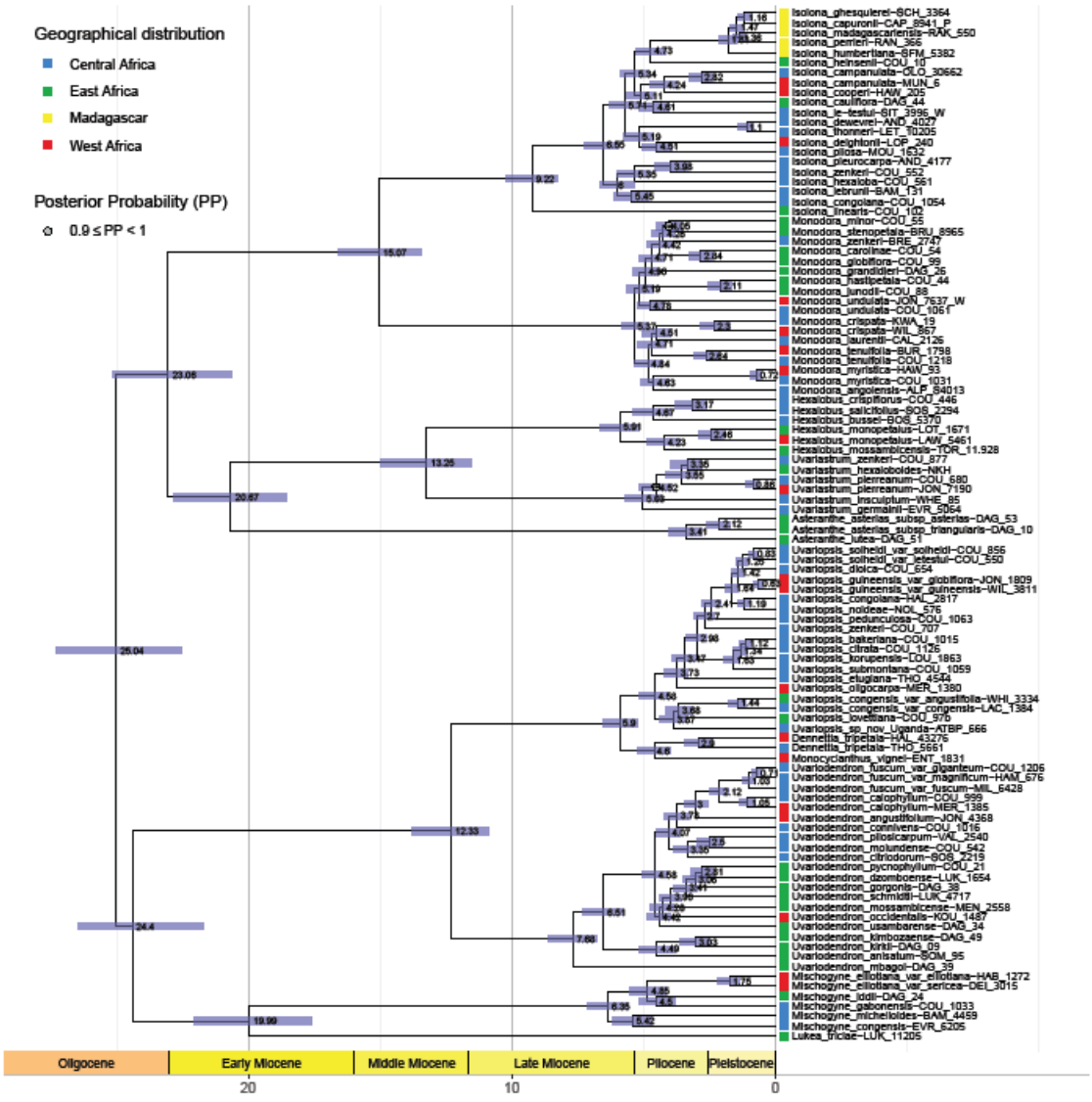

1287

1288 Fig. 2: Phylogenetic tree of the Monodoreae specimens, as pruned from the Maximum
1289 Credibility Clade tree estimated from 8,601 posterior tree inferred on 32 nuclear loci with
1290 uncorrelated molecular clock and fossil calibration in BEAST. The value at the node indicates
1291 the mean age from the posterior probability density, and the blue bar indicates the 95%
1292 highest posterior density interval of the age. All nodes received a posterior probability of 1
1293 except for those indicated by a grey circle. The colour square at the tip indicates the
1294 geographic origin of the specimen. Colours follow Fig. 1.

1295

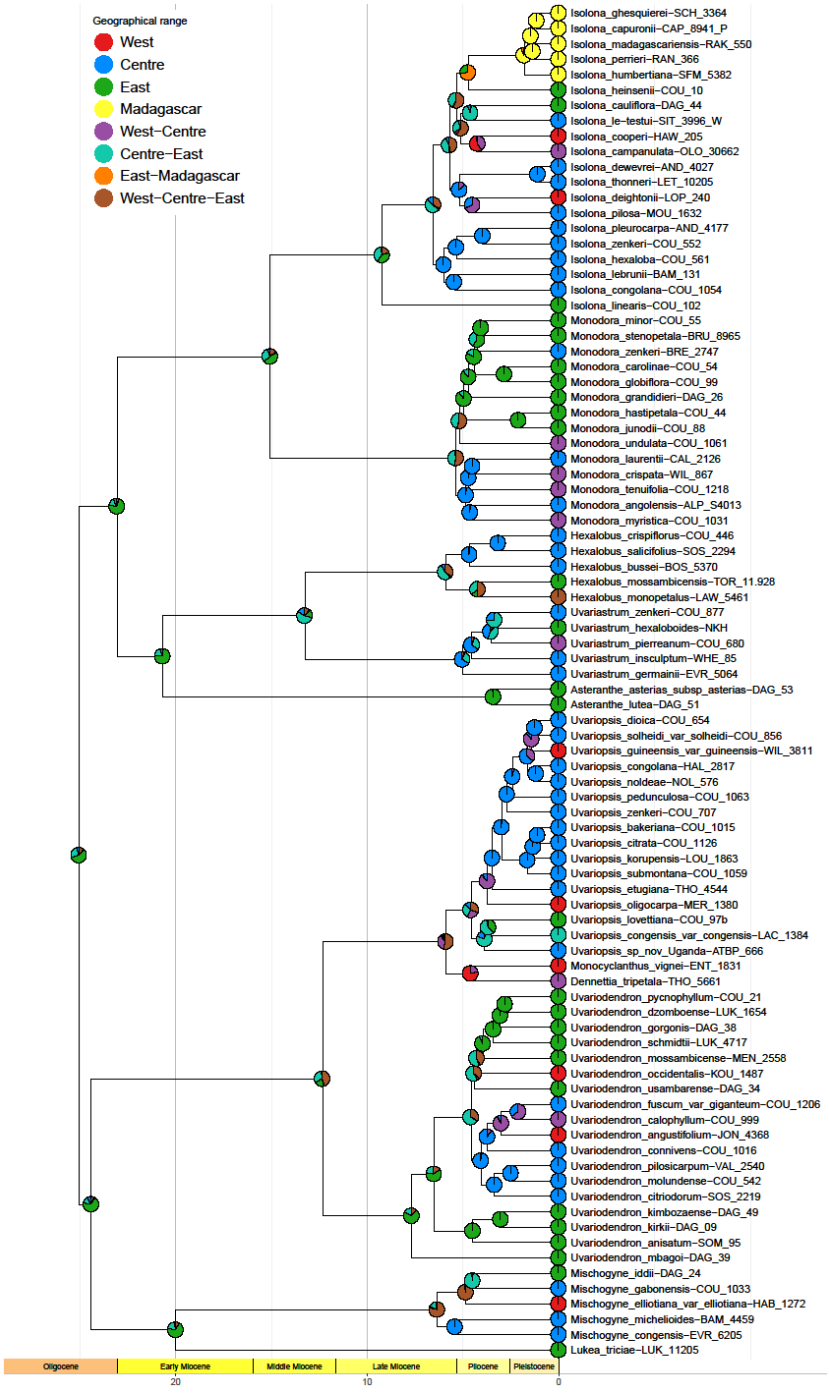

1296

1297 Fig. 3: Phylogenetic tree of the Monodoreae species, as pruned from the Maximum
1298 Credibility Clade tree estimated from 8,601 posterior tree inferred on 32 nuclear loci with
1299 uncorrelated molecular clock and fossil calibration in BEAST, with present day (next to
1300 names) and ancestral ranges (pies at the internal nodes) reconstructed using the dispersal–

extinction–cladogenesis (DEC) analysis implemented in BioGeoBEARS. The relative proportions of the coloured slices in the pies are proportional to the likelihood of each state.

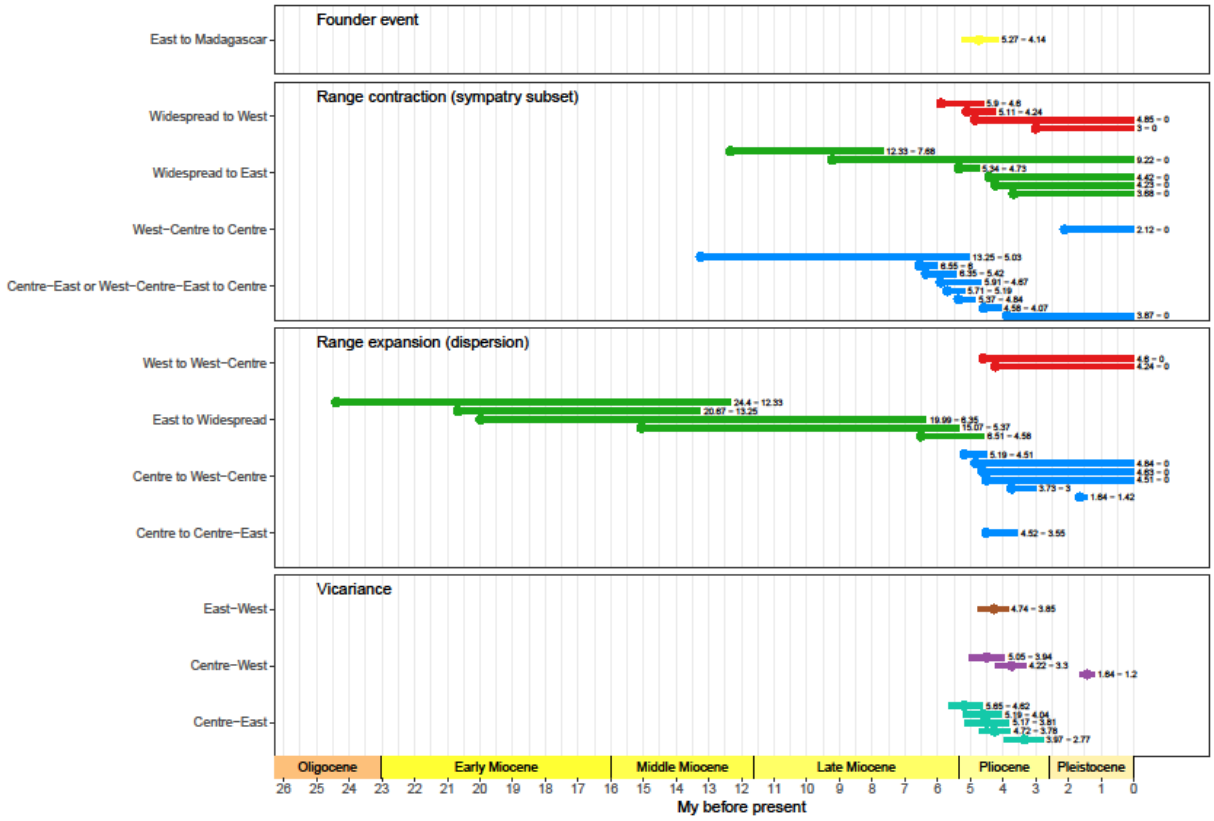

Fig. 4: Chronological time frame of the biogeographical events as interpreted from the DEC model. The founder event and vicariance events occurred at nodes of the tree in Fig. 3: the dot and horizontal bar represent the mean age and 95% highest posterior density interval of the age of the node, respectively. Range contraction (RC) and range expansion (RE) events occurred along branches connecting two nodes: the dot represents the mean age of the widespread (RC) or endemic (RE) ancestral node, and the horizontal bar extends toward the mean age of the endemic (RC) or widespread (RE) daughter node. Colours follow the dispersal–extinction–cladogenesis ranges (see Fig. 3) and have different meaning depending on the event: for founder event, it is the colour of the range after the founder event; range contraction, it is the colour of the endemic range after range contraction; range expansion, it is

the colour of the endemic range before range expansion; vicariance, it is the colour of the widespread range before the vicariance event. The labels on the y-axis indicate the direction of the event (e.g. range expansion from East to Widespread). 'Widespread' includes all the widespread ranges (West-Centre, Centre-East or West-Centre-East). See Material and Methods for the details on the events.

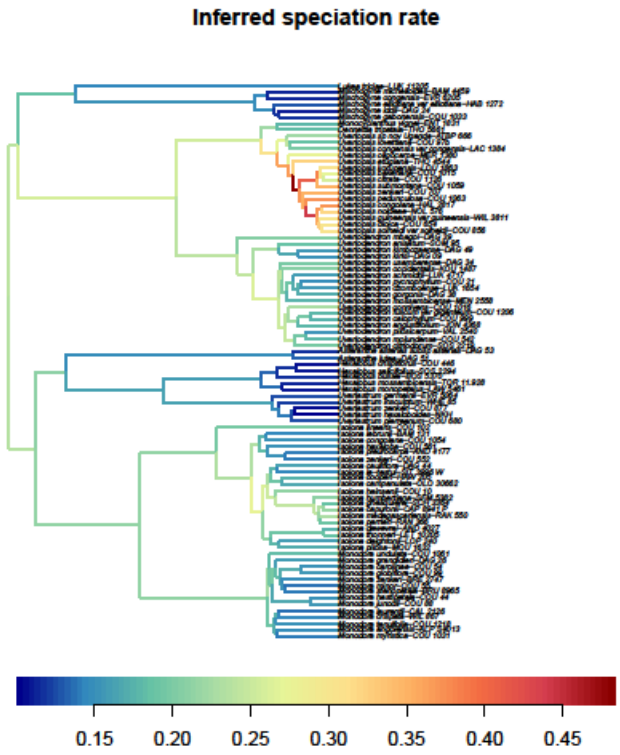

Fig. 5: Species-specific speciation rates through time of Monodoreae estimated using ClaDS (event per Myr).

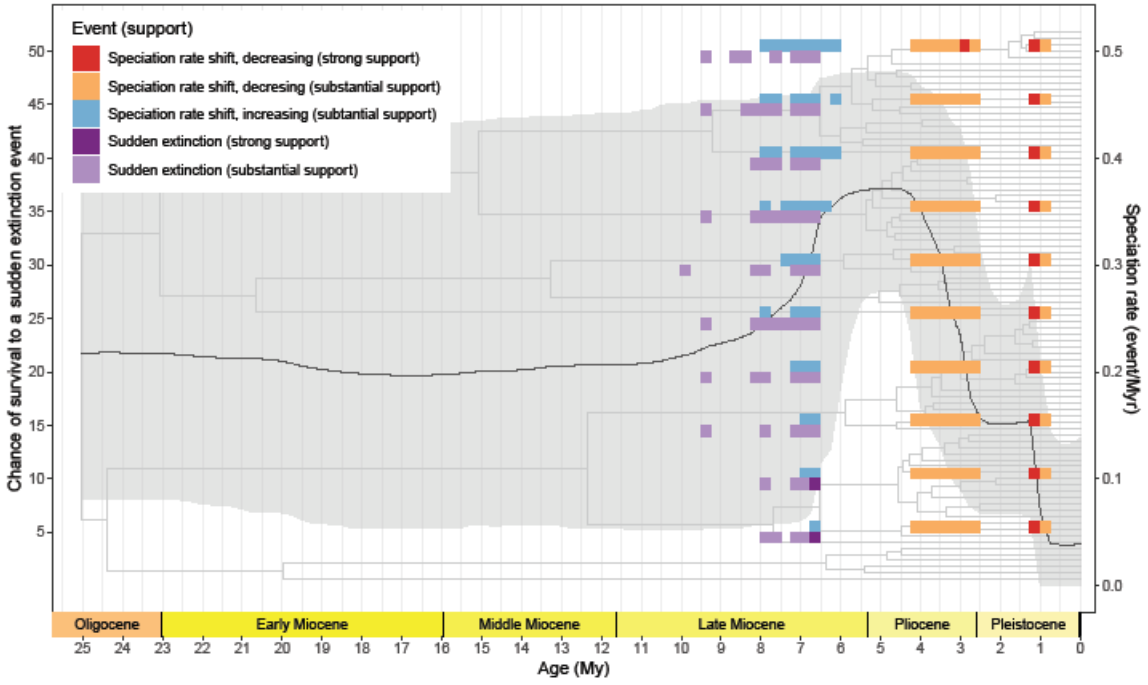

1323

1324 Fig. 6: Summary of speciation rate shifts and sudden extinction (ME) events at each time slice
1325 in the CoMET analysis, with the priors on the chance of survival to a sudden extinction event
1326 (ME) ranging from 5% to 50% (Fig. S7 – Fig. S16 [**Supplementary Information**]). Strong
1327 support indicates 2lnBF > 6 in, substantial support indicates 2lnBF > 2. Black line represents
1328 the speciation rate and grey shading its 95% credibility interval, both averaged from all the
1329 CoMET analyses (Fig. S7 – Fig. S16 [**Supplementary Information**]).

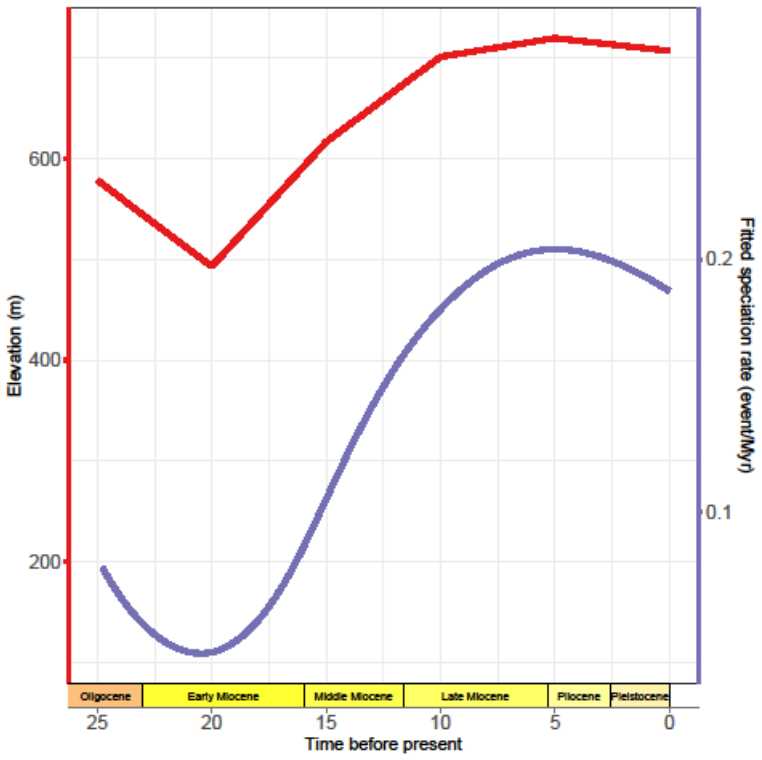

1330

1331 Fig. 7: Clade-independent speciation rate through time of Monodoreae, as estimated in

1332 RPANDA with the speciation rate varying exponentially with the mean elevation of tropical

1333 Africa through time (BElev model, Table 1).

1334

1335

Tables

Table 1. Results of the environment-dependent birth-death models applied to the Monodoreae with RPANDA. When the rates are not constant, they vary exponentially with time or with the environmental variables (temperature = Temp, or elevation = Elev, or percentage of C4 plants = PercC4). logL, log-likelihood; λ0, speciation rate; α, rate of variation of the speciation according to the paleo-environmental variable; μ0, extinction rate; β, rate of variation of the extinction according to the paleo-environmental variable.

Model	Speciation varies with:	Extinction varies with:	logL	AICc	λ_0	α	μ_0	β	ΔAICc
BDPercC4	C4 proportion	C4 proportion	-224.08	456.63	1.6829	-0.0439	2.1736	-0.0656	-12.66
BElev	elevation	no extinction	-232.57	469.29	0.0017	0.0066	-	-	0
BElevDConst	elevation	constant	-232.63	471.55	0.0029	0.0059	0.0005	-	2.26
BTemp	temperature	no extinction	-234.17	472.48	0.1255	0.0829	-	-	3.19
BConst	constant	no extinction	-235.75	473.55	0.1797	NA	-	-	4.26
BPercC4	C4 proportion	no extinction	-234.83	473.81	0.2396	-0.0072	-	-	4.52
BConstDPercC4	constant	C4 proportion	-234.06	474.41	0.1963	NA	0.3638	-0.0958	5.12
BTempDConst	temperature	constant	-234.17	474.62	0.1254	0.083	0	-	5.33
BTime	time	no extinction	-235.67	475.49	0.1865	-0.0072	-	-	6.2
BDConst	constant	constant	-235.75	475.63	0.1796	NA	0	-	6.34
BPercC4DConst	C4 proportion	constant	-234.83	475.96	0.2396	-0.0072	0	-	6.67
BDTemp	temperature	temperature	-234.17	476.82	0.1255	0.0829	0	0.0156	7.53
BTimeDConst	time	constant	-235.67	477.63	0.1864	-0.0071	0	-	8.34
BConstDTime	constant	time	-235.75	477.78	0.1797	NA	0	-0.0499	8.49
BConstDElev	constant	elevation	-235.75	477.79	0.1797	NA	0.0809	-0.0781	8.5
BConstDTemp	constant	temperature	-235.75	477.79	0.1796	NA	0	-0.0016	8.5
BDTime	time	time	-235.67	479.83	0.1865	-0.0072	0	0.0259	10.54
BDElev	elevation	elevation	-236.44	481.36	0.2674	-0.0005	0	0.0022	12.07